OVERLAND FLOW PARTITIONING FOR RILL AND INTERRILL EROSION MODELING

by

Donna Ingram Page

A Thesis Submitted to the Faculty of the

SCHOOL OF RENEWABLE NATURAL RESOURCES

In Partial Fulfillment of the Requirements
For the Degree of

MASTER OF SCIENCE
WITH A MAJOR IN WATERSHED MANAGEMENT

In the Graduate College

THE UNIVERSITY OF ARIZONA

1 9 8 8

STATEMENT BY AUTHOR

This thesis has been submitted in partial fulfillment of requirements for an advanced degree at The University of Arizona and is deposited in the University Library to be made available to borrowers under rules of the Library.

Brief quotations from this thesis are allowable without special permission, provided that accurate acknowledgment of source is made. Requests for permission for extended quotation from or reproduction of this manuscript in whole or in part may be granted by the head of the major department or the Dean of the Graduate College when in his or her judgment the proposed use of material is in the interests of scholarship. In all other instances, however, permission must be obtained from the author.

SIGNED: Donna L. Page

APPROVAL BY THESIS DIRECTORS

This thesis has been approved on the date shown below:

Leonard J. Lane — July 12, 1988
LEONARD J. LANE — Date
Adjunct Professor of Watershed Management

Martin M. Fogel — July 7 1988
MARTIN M. FOGEL — Date
Professor of Watershed Management

Richard H. Hawkins — July 14, 1988
RICHARD H. HAWKINS — Date
Professor of Watershed Management

ACKNOWLEDGMENTS

I would first like to express my gratitude to Dr. Leonard J. Lane. Over the past 18 months he has taught me the fundamentals of erosion science and has given me the opportunity to work on many different aspects of the Water Erosion Prediction Project (WEPP). I could not have completed this work without his encouragement and guidance.

I would like to thank Dr. Mark A. Nearing for his expertise, guidance, and patience over the course of this study. I also want to thank my graduate committee members, Dr. Martin M. Fogel and Dr. Richard H. Hawkins, for their time and suggestions. I extend a special thanks to Dr. Donald F. Post for introducing me to the study of erosion and to the people involved in the WEPP.

I wish to thank Roger Simanton and Dr. John Laflen for providing the field data and for the opportunity to assist in the field experiments for rangelands and croplands. I want to thank the entire rangeland and cropland field crews for their excellent work in conducting the field experiments and for making the field work fun.

I would like to acknowledge the contributions of the entire staff of the Aridland Watershed Management Research Unit of the U. S. Department of Agriculture's Agricultural Research Service which provided computer facilities and technical assistance. I especially want to thank Sue Anderson, Laura Yohnka, and Wade Taul for their guidance in the preparation of this manuscript.

Finally, I wish to thank my friends and family for their support and encouragement during the course of my studies at the University of Arizona.

TABLE OF CONTENTS

TABLE OF CONTENTS--Continued

LIST OF ILLUSTRATIONS

LIST OF ILLUSTRATIONS--Continued

LIST OF TABLES

ABSTRACT

Accurate estimation of the shear stress of flowing water is important in modeling rill and interrill erosion. The shear stress of flow in rills helps determine detachment capacity and transport capacity of flow. This study investigated shear stress estimation in erosion modeling.

Rill shear stress estimates based on sheet flow and on flow partitioned into rill and interrill areas for a uniform slope were compared. It was found that the sheet flow assumption underestimated actual shear stress in rills.

Estimates of rill spacing and rill width affect shear stress in rills. It was found that increasing the distance between rills could increase predicted sediment loads while sediment loads reached a maximum then decreased for increased rill widths.

Erodibililty parameters for an erosion model were found using optimization. Optimal values for rill erodibility parameters were found to be distorted when based on a model that estimated shear stress from sheet flow.

CHAPTER 1

INTRODUCTION

Background

Erosion of soil by the action of wind and water is a natural process which is often accelerated by human activities. Erosion, especially by water, has several far-reaching consequences. Water erosion is a major problem in many cultivated and rangeland areas where the nutrients are removed by the water along with the sediment, leaving soils shallower and less productive. Erosion can cause water quality problems when the sediment entrained in the flow is deposited in lakes and rivers. Water erosion has become increasingly important with the expanded use of chemicals on the land. Chemical and biological pollutants are transported by water with the sediment to distant locations (non-point source pollution).

To help evaluate these problems, the field of erosion science has evolved to predict the amount of erosion caused by water under different circumstances. In order to make responsible decisions about land use, accurate erosion prediction models are important tools in identification of erodible soils and in planning management strategies that can mitigate the effects of water erosion.

Currently, the most widely used erosion model is the Universal Soil Loss Equation (USLE) (Wischmeier and Smith, 1978). The USLE is an empirically based model designed to predict long term average annual soil loss from water erosion from specific fields with certain cropping and management systems. Because of the empirical nature of the model, it is difficult to apply it to many Western soils and to rangelands in the absence of on-site data. Scientifically, the USLE is considered

mature technology with limited potential for major improvements (Foster and Lane, 1987).

Recent advances in the fields of hydrology and erosion science have resulted in the development of physically based equations for the processes related to erosion by water. These equations have provided the basis for developing improved prediction models of erosion. The U.S. Department of Agriculture-Agricultural Research Service (USDA-ARS) is currently involved in a major effort to develop a process-based model of water erosion to replace the USLE.

One of the processes important to the model is the detachment of soil by flowing water. In areas of concentrated flow, sediment detachment depends, in part, on the shear stresses acting on the soil. The method of shear stress estimation is important since it affects the estimates of detachment rates. Because the shear stress estimates affect the estimates of sediment detachment, they also affect estimates of soil erodibility parameters. These soil erodibility parameters are needed to accurately model soil erosion by water. This research to investigate shear stress estimation and erodibility parameters was conducted as part of the USDA's Water Erosion Prediction Project (WEPP).

Review of Literature

Erosion

The erosion caused by surface runoff is usually classified into four stages that correspond to increasing flow concentration (Foster et al., 1977; Hudson, 1981). They are referred to as interrill, rill, gully, and stream channel erosion.

In the initial phase of surface runoff, water moves downslope over the land surface and is termed overland flow (Horton, 1945). Overland

flow often concentrates into small definable channels called rills (Foster, 1971). Rill erosion is caused by the flow in these rills. Interrill erosion takes place on the areas between rills as a result of raindrop impact and shallow overland flow. The term upland erosion is used for the overland flow processes of interrill and rill erosion (Foster, 1982).

As surface runoff concentrates into gullies and stream channels the hydraulic forces of the flow cause erosion. Gullies often are defined as small channels that, unlike rills, cannot be eliminated by normal tillage (Hudson, 1981). Stream channels are larger and more permanent than gullies. Together they are considered channel flow.

All four types of erosion may contribute to the total erosion in a typical watershed. The first step in modeling the erosion process from a watershed is to describe the erosion from upland areas. The contributions from upland areas can then be delivered to the channel flow components.

The model used in this study is designed to estimate upland erosion from interrill and rill areas. Meyer and Wischmeier (1969) have identified the four subprocesses involved in upland erosion as: detachment by rainfall, transport by rainfall, detachment by runoff, and transport by runoff. In order to accurately model erosion from these two sources, it is important to understand where these subprocesses occur and their relative importance.

Interrill Erosion

Interrill erosion primarily involves the processes of detachment by rain and transport by thin sheet flow (Foster and Meyer, 1975; Meyer et al., 1975a). Meyer et al. (1975a) found that detachment by raindrop

impact accounted for over 90% of the soil loss from small soil pans. Detachment of soil particles by interrill flow was found to be negligible compared to that of raindrop impact (Young and Wiersma, 1973) because of the low shear stresses found in thin sheet flow. Detachment by raindrop impact is related to both the characteristics of the rain and of the soil.

Transport of detached soil particles from interrill areas to rills occurs mainly by thin sheet flow. Several studies have shown that direct splash of detached particles into rills is very small compared to that transported by interrill flow (Young and Wiersma, 1973; Lattanzi et al., 1974; Meyer et al., 1975a). Rainfall can increase the transport capacity of the flow by creating turbulence that can lift particles into the flow (Foster and Meyer, 1975). This can be important on slopes with very small gradients where the transport capacity of the flow can limit the movement of detached particles (Foster, 1982).

Rill Erosion

The two dominant subprocesses involved in rill erosion are detachment and transport by rill flow (Foster and Meyer, 1975). Detachment and transport by rain are not usually considered factors in rill erosion although rainfall could increase transport capacity by rill flow (Foster, 1982).

Rills form when irregularities of the soil surface cause overland flow to concentrate. The shear stress of this concentrated flow is higher than that of thin sheet interrill flow. If the shear stress exceeds the soil's critical shear stress, it will begin to detach particles at positions in the flow where shear stress is greatest

(Foster, 1982). Evidence for the existence of a threshold (critical) shear stress for erosion to begin was described by Meyer et al. (1975b).

A rill will deepen until it reaches a less erodible boundary. At this point, it will widen and the erosion rate will decrease. A simple model of this process has been found to reproduce observed sediment yield and hydraulic geometry from a rill erosion study (Lane and Foster, 1980b).

Rill erosion has been described as a combination of three subprocesses: local erosion around headcuts, shear erosion around the wetted perimeter of the rill, and undercut erosion of material that has slumped into the rill from undercut sides (Meyer et al., 1975b).

The erosion caused by each of these subprocesses depends directly on the hydraulics on flow in the rill. A detailed analysis of rill hydraulics by Foster et al. (1984a; 1984b) has shown large variations of velocity, flow depth, and shear stress around the wetted perimeter and along the length of a rill both in time and space. These variations cause locally intense shear stresses that accelerate erosion and sediment transport.

Conceptually, total shear stress from flow in a rill is made up of stresses from form roughness and grain roughness. (Graf, 1971). Erosion and sediment transport is considered to be the result of grain roughness while form roughness affects the rill hydraulics. It has been proposed that a stochastic model that accounts for the spatial and temporal variations of rill hydraulics could improve rill erosion estimates (Foster et al. 1984b). Currently, since the mechanics of the rill subprocesses are not well understood, the modeling of rill erosion is usually related to average shear stress of the flow in the rill.

The ability of rill flow to detach particles depends on the transport capacity of the flow in addition to shear stress of the flow and soil properties. If the flow's transport capacity is partially filled by incoming interrill sediment or rill flow detachment, the rill erosion rate decreases (Foster and Meyer, 1972). When the sediment load is greater than the transport capacity, deposition occurs.

Transport capacity has been described by a number of relationships in rill erosion models. These include the Peter-Meyer equation (Rohlf and Meadows, 1980) and the DuBoys equation (Young and Mutchler, 1969). Foster and Meyer (1972) proposed the use of a simplified form of the Yalin equation that depends on the shear stress of the flow and the transportability of the sediment for erosion modeling. This approach was shown to accurately fit observed data over a range of typical overland flow conditions (Foster, 1982).

Factors That Affect Interrill and Rill Erosion

The influence of factors, such as slope gradient and surface cover, on erosion were observed as early as the 1940's (i.e. Zingg, 1940; Smith, 1941). Models such as the USLE (Wischmeier and Smith, 1978) and CREAMS (Knisel, 1980) have attempted to account for them. The effects of these factors on rill and interrill erosion can be very different depending on the subprocesses they influence.

The effect of slope steepness on erosion rates was found to be small for interrill areas compared to rills (Watson and Laflen, 1986; Meyer et al. 1975a, Lattanzi et al., 1974). In rills, increased slope steepness results in higher shear stresses in the flow that lead to higher detachment rates. The small increase in erosion in that is seen in interrill areas has been attributed to increased detachment by higher

raindrop impact angle and easier transport down steep slopes (Lattanzi et al. 1974).

Increased slope length has been shown to increase rill erosion (i.e. Gilley, 1987) while the same effect was not seen in interrill erosion (Lattanzi et al., 1974). This is the result of increased flow concentrations with distance downslope that increase shear stress in rills. This is not found in interrill areas since detachment is mainly by raindrop impact.

The effect of increasing surface cover in reducing interrill erosion has been shown many times including studies by Lattanzi et al. (1974) and Gilley et al. (1986b). Increased surface cover limits the amount of interrill soil exposed to raindrops and absorbs some of the energy of their impact. This effect has also been found for increased canopy cover on interrill areas (i.e. Foster, 1982).

Rill erosion has also been found to decrease with increased surface cover (i.e. Gilley et al., 1986a; 1986b). In rills, the surface cover reduces the shear stress acting on the soil. Incorporated crop residue has also been found to decrease shear stress of flow and rill erosion (Brown, 1988).

Optimization of Parameter Values

Current erosion models are based on parametric equations that describe the erosion process. Accurate estimation of the parameter values involved is an essential part of model development. The erosion model described by Lane et al. (1987) includes a differential sediment load equation to model quasi-steady state erosion. Since this equation cannot be solved analytically, erosion parameters cannot be directly obtained. In addition, parameter estimation from regression techniques

with field data requires simplifying assumptions can that distort true parameter values (Nearing et al. unpublished manuscript).

Another technique used to identify parameter values is optimization. Optimization involves finding the parameter values that will best predict observed data. This technique has often been used to find parameters for rainfall-runoff models (i.e.. Sorooshian and Arfi, 1982). More recently it has been applied to erosion modeling to find erodibility parameters (Blau et al., 1988; Brown, 1988; and Nearing et al., unpublished manuscript). Blau et al. (1988) found that for the three parameter dynamic erosion model used (Shirley and Lane, 1978) there was a large variation in parameter estimates due to parameter insensitivity. Nearing et al.'s investigation of the rill erodibility parameters in the WEPP model, found fewer problems with parameter identifiability.

Problem Statement and Objectives

Accurate estimates of shear stress are important in process-based erosion modeling because the detachment of soil particles is partially based on the tractive force or shear stress of the flow on the soil. Past estimates of shear stress were often based on the assumption of uniform sheet flow for both interrill and rill areas (i.e. Rowlinson and Martin, 1971). Comparison of shear stress estimates for various concentrated and overland flow conditions show that this does not accurately represent the situation. The shear stress in rills can be much greater because of the concentration of flow. When rills are present, underestimation of shear stress could lead to underestimation of the sediment yield.

This study was designed to examine this problem of shear stress estimation and its effect on modeling soil loss and sediment load. It was carried out in three parts. The first part involved quantifying the difference in rill shear stress estimated from uniform sheet flow and that estimated from concentrated flow. A program that made these calculations was written and run for different flow conditions (rill width, slope gradient, rill geometry, etc.).

Next, a sensitivity analysis was performed to examine the effect of rill spacing and rill width on predicted sediment loads. The distance between rills and the width of the rill affect the shear stress of the rill flow and therefore, the detachment of sediment. The WEPP erosion model was used to predict sediment loads for various conditions.

The third phase of the study was undertaken to compare the effects of using shear stress estimates based on uniform sheet flow and those based on flow partitioned into rill and interrill areas in the WEPP erosion model. The effects were quantified by examining the rill and interrill erodibility parameters for the two cases. The parameter estimates were obtained by optimization techniques using field data from rainfall simulator experiments from cropland and rangeland sites. The optimization uses the same relationships for overland flow routing and erosion that are used in the current USDA-WEPP modeling effort.

CHAPTER 2

MODEL DESCRIPTION

Description of the WEPP Model

The model used in this study is the USDA-WEPP model currently being developed to replace the USLE. The model is designed to estimate soil erosion caused by rainfall and surface flow on field size areas (up to 250 hectares). WEPP is being developed for use by action agencies that are dealing with soil erosion problems.

To be a practical tool for field work, the model must be easy to use and teach to others, be applicable to a broad range of conditions, and have a short computational time on a personal computer. Reduction of computation time is achieved by assuming quasi-steady state conditions and using analytical solutions whenever possible (Foster et al. 1987).

The following is a brief presentation of the equations that describe processes of overland flow, detachment, transport, and deposition that are used in the WEPP model. A more detailed description of the equations and their use in this model is given by Lane et al. (1987).

Overland Flow Routing

The mathematical description of the movement of overland flow down a hillslope is called routing. Overland flow is one of the main components of the erosion process in its ability to detach and transport soil particles. Hydraulically, overland flow is considered unsteady, nonuniform flow since it varies in depth and velocity over time and space. The two hydrodynamic principles describing this flow are conservation of mass (continuity) and the momentum equation.

Woolhiser and Liggett (1967) showed that on most overland flow planes, routing with the kinematic wave approximation to overland flow was valid. Kinematic flow occurs when there is a balance between gravitation and friction forces. These conditions result in the simplification of the momentum equation to (Freeze, 1978):

$$S_o = S_f \tag{1}$$

where: S_o = bed slope (dimensionless)

S_f = friction slope (dimensionless)

and the continuity equation to:

$$\frac{dh}{dt} + \frac{dq}{dx} = r - i_f \tag{2}$$

where: h = local depth of flow (L)

t = time (T)

x = distance in flow direction (L)

r = rainfall rate ($L^3/T/L^2$)

i_f = infiltration rate ($L^3/T/L^2$)

$$q = \alpha h^m \qquad (L^2/T) \tag{3}$$

with α and m as the parameters of the depth-discharge equation. The quantity $(r - i_f)$ is called the rainfall excess rate (RE).

Equation 3 is a depth-discharge equation based on uniform flow formulas. It considers overland flow as a broad thin sheet, like a wide channel, with the width very large in relation to the depth so that well-established channel flow equations (Chezy or Manning) may be used to evaluate the parameters. Using the Chezy equation, the exponent m in equation 3 is 3/2 and the coefficient may be expressed as:

$$\alpha = CS^{1/2} \tag{4}$$

where: C = Chezy resistance coefficient ($L^{1/2}/T$)

$$= (8g/f)^{1/2} \tag{5}$$

g = acceleration of gravity (L/T^2)

f = Darcy-Weisbach friction factor (dimensionless)

S = slope (dimensionless).

The total hydraulic resistance, as represented by the friction factor f, is:

$$f = f_{soil} + f_{rr} + f_{cov} \tag{6}$$

where f_{soil} is the friction factor of flow on bare soil, f_{rr} is the friction factor due to the random roughness of the flow surface, and f_{cov} is friction factor from cover in direct contact with the soil surface. This division of resistance was derived using sediment transport theory (Graf, 1971).

On a hillslope, overland flow often concentrates in rills. The steady state flow in rills may be described by the Chezy channel flow equation as:

$$q = CS^{1/2}R^{3/2} \tag{7}$$

where: R = hydraulic radius

$$= \frac{\text{cross sectional area perpendicular to flow}}{\text{wetted perimeter.}} \tag{8}$$

The use of the hydraulic radius in the equation for rill flow accounts for the role the channel sides play in flow resistance.

Success in modeling overland flow is dependent on how accurately the actual land surface is described. Until now, most models have based the flow equations on broad uniform sheet flow. Lane and Woolhiser (1977) have shown that this assumption results in distortions of the model parameters. This distortion depends on how irregular the land surfaces really are. It is therefore important to partition flow into sheet and rill flow to minimize the distortions in the model parameters and to better represent the actual flow conditions.

Erosion Equations

Upland erosion modeling is based on the concept that the sediment load is controlled by either the amount of sediment available for transport by detachment or by the transport capacity of the flow (Meyer and Wischmeier, 1969; Foster, 1982).

Continuity Equation

Quantitatively, the erosion calculations are based on the steady state sediment continuity equation (Foster and Meyer, 1972):

$$\frac{dG(x)}{dx} = D_i + D_f(x) \tag{9}$$

where: x = distance downslope (L)

$G(x)$ = sediment load at x (M/T/L)

D_i = interrill erosion rate ($M/T/L^2$) and

$D_f(x)$ = rill erosion rate ($M/T/L^2$).

D_f is positive when there is detachment and transport and negative when there is deposition.

Interrill Erosion

Total interrill detachment, as described earlier, is a result of raindrop impact and detachment by thin sheet flow. Since the detachment by water flow may be very small relative to raindrop impact the interrill erosion is assumed to be adequately represented by the relationships outlined by Foster (1982) and modified for this model (Lane et al., 1987) by the equation:

$$D_i = C_i K_i I^2 \tag{10}$$

where: C_i = interrill cover parameter (dimensionless)

K_i = interrill soil erodibility parameter (MT/L^4) and

I = rainfall intensity (L/T).

The parameter C_i is a function of the canopy height and the fraction of the soil surface covered by the canopy and material in direct contact with the ground surface. K_i depends on soil properties. D_i is considered to be independent of x (downslope distance).

Rill Erosion

Erosion in rills is modeled as a function of the ability of the flow to detach soil particles and its ability to transport them once they are detached. If the sediment load of the flow is less than its capacity to transport sediment and the flow has sufficient force, detachment occurs. Net rill detachment is described by Foster and Meyer (1972, 1975) as:

$$D_f = D_c(x)\ [1-\frac{G(x)}{T_c(x)}] \tag{11}$$

where: D_c = detachment capacity of the flow ($M/L^2/T$)

T_c = transport capacity of the flow (M/L/T).

Detachment capacity is expressed as:

$$D_c = K_r[\tau(x) - \tau_c(x)] \tag{12}$$

where: K_r = rill soil erodibility parameter (T/M)

$\tau(x)$ = shear stress of flow acting on the soil (F/L^2)

$\tau_c(x)$ = rill detachment threshold parameter (F/L^2).

The parameter $\tau_c(x)$ is the critical shear stress of flow required for detachment to occur.

Transport capacity is estimated using the Yalin sediment transport equation as modified by Foster (1982) to account for the transport capacity for various particle sizes and densities. The approximate equation used for transport capacity in the WEPP model is:

$$T_c = K_t\tau^{3/2} \tag{13}$$

where: K_t = coefficient (T/L^2)

τ = average flow shear stress acting on the soil (F/L^2).

The coefficient K_t is calibrated from the actual transport capacity at the end of the slope. The actual transport capacity is calculated using the modified Yalin equation described earlier.

When the sediment load is greater than the transport capacity, net deposition occurs. Deposition, as described by Foster and Meyer (1975), is calculated as:

$$D_f(x) = D_r(T_c(x) - G(x)) \tag{14}$$

where: D_r = depostition rate parameter $(M/L^2/T)$.

The detachment parameter is found by the equation:

$$D_r = \beta V_f/q(x) \tag{15}$$

where: β = dimensionless parameter

V_f = particle fall velocity (L/T) and

$q(x)$ = discharge flow rate per unit width (L^2/T).

The factor β represents the turbulence effect of raindrop impact on flow that delays the deposition of sediment.

Shear Stress Equations

The equation for total shear stress in overland flow on a plane is:

$$\tau = \gamma hS \tag{16}$$

where: τ = total shear stress (F/L^2)

γ = weight density of water (F/L^3)

h = depth of flow (L)

S = slope (dimensionless).

For stress in concentrated flow, the equation becomes:

$$\tau = \gamma RS \tag{17}$$

where R is the hydraulic radius (Equation 8). Calculations for R depend on knowing or assuming a channel geometry.

CHAPTER 3

METHODS

The relationships described above show the importance of the shear stress estimates in determining the detachment capacity and the transport capacity of flow in rills for erosion modeling. The effect of shear stress estimation on erosion modeling was investigated three ways. The first was comparison of the shear stress values calculated for different flow conditions for shear stress estimated from sheet flow and from rill flow. Next, the effects of rill spacing and rill width, which both affect rill shear stress, on sediment loads predicted from the WEPP erosion model were examined. Finally, the baseline parameter values for interrill and rill erodibility and critical shear stress (K_i, K_r, and τ_c respectively) obtained by optimization from rainfall simulator data were examined. Each data set was optimized for erosion calculations based on shear stress from sheet flow and shear stress from rill flow.

Shear Stress on a Uniform Slope

The initial phase of the investigation consisted of the calculation of shear stress on a uniform slope when the flow was considered uniform sheet flow and when it was partitioned into rill and interrill areas. A program was written that partitioned the flow according to the angle of water flow into the rill (Fig. 1) and then calculated shear stress at various distances down a unit width (1-m) slope. The flow was considered to increase linearly downslope with the rainfall excess rate:

$$q = RE * x \tag{18}$$

where: q = flow rate (m^2/s)

RE = rainfall excess rate (m/s)

x = distance downslope (m).

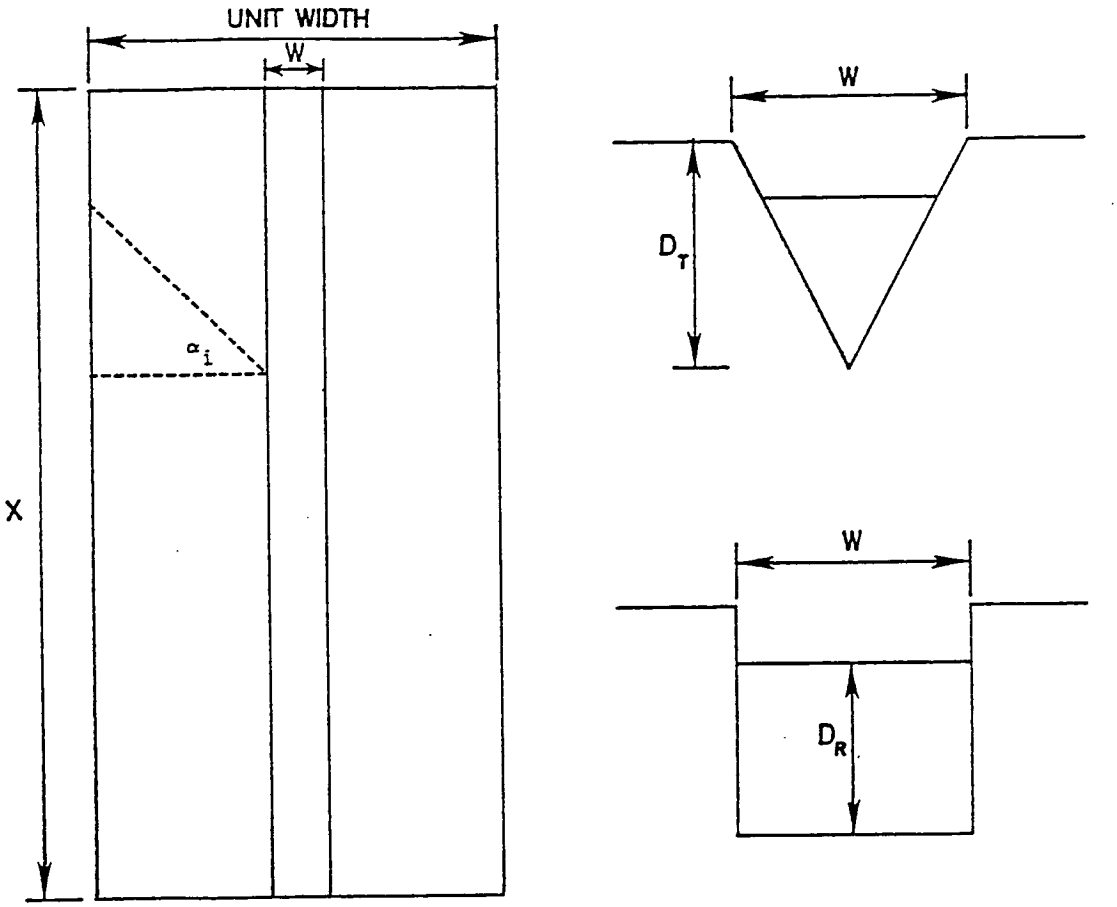

Figure 1. Representation of slope and rill geometries for shear stress on uniform plane study. a) A uniform slope with one rill. W = width of rill, α_i = angle of inflow to rill, and X = distance downslope b) geometry of a triangular rill (D_T =depth of triangular rill) and c) geometry of rectangular rill (D_R=depth of water in rectangular rill).

The model was run for a 100-m slope length and two different rill geometries: triangular and rectangular. Shear stress values were obtained for different rill widths, angles of flow into the rill, and slope gradients for both rill geometries. For triangular rills, the depth of the rill was also varied because of its importance in determining the hydraulic radius.

Effect of Rill Spacing and Rill Width

The second part of this study investigated the effects of varying the distance between rills and the rill width on sediment loads predicted with the WEPP erosion model. The horizontal distance between rills is referred to as the rill spacing.

The erosion model assumes a rectangular rill geometry for the estimation of hydraulic radius and shear stress for the rill flow. The width of the rill was found by relating it to the discharge with the relationship used in the CREAMS model (Lane and Foster, 1980a) and modified for metric units:

$$W = aQ^b \tag{19}$$

where: W = width (L)

Q = discharge in the rill (L^3/T)

$a = 4.39$

$b = 0.5$

Given the discharge, Q, and the width, W, the depth of steady, uniform flow (normal flow) was calculated using a numerical procedure.

The effect of the rill spacing was examined by running the model for a 50-m, 5%, slope for four different rill spacings. Each rill spacing was run with three different τ_c and K_i values and two rainfall

intensities. Predicted sediment loads were obtained for each intensity with each combination of rill spacing, τ_c and K_i.

The sensitivity of the model to rill width was tested by changing the value of the coefficient (a) in the rill width estimation equation (Equation 19). The model was run for the same set of variables as the rill spacing study (the same K_i and τ_c values and rainfall intensities) with rill spacing set at 1-m. Four different values for the coefficient were tested: 2, 4.39, 6, and 8. Predicted sediment loads were found for each rill width. Results of these tests are discussed in Chapter 4.

Optimization of Erosion Model Parameters

Field Data Collection Methods

Rainfall simulator experiments are being performed to assist in the evaluation of the soil erodibility parameters in the WEPP erosion model. A wide range of cropland soils, located throughout the United States, and rangeland soils from the Western U. S. are being tested. A rotating boom rainfall simulator developed by Swanson (1965) is used for both croplands and rangelands. Methods for croplands and rangelands will be discussed separately since they are slightly different.

Croplands

A cropland site consisted of six preformed rills and ten small interrill plots (Fig. 2) on an area that had been plowed and disked before plot installation. Rills were about 6 cm deep and 9 m long and spaced about 0.48 m apart. Interrill plots were 0.75 m x 0.50 m.

The rainfall simulation procedure was outlined by Laflen et. al. (1987). In the initial run, rain was applied at a rate of about 60 mm/hr until runoff was constant. During this time, samples were

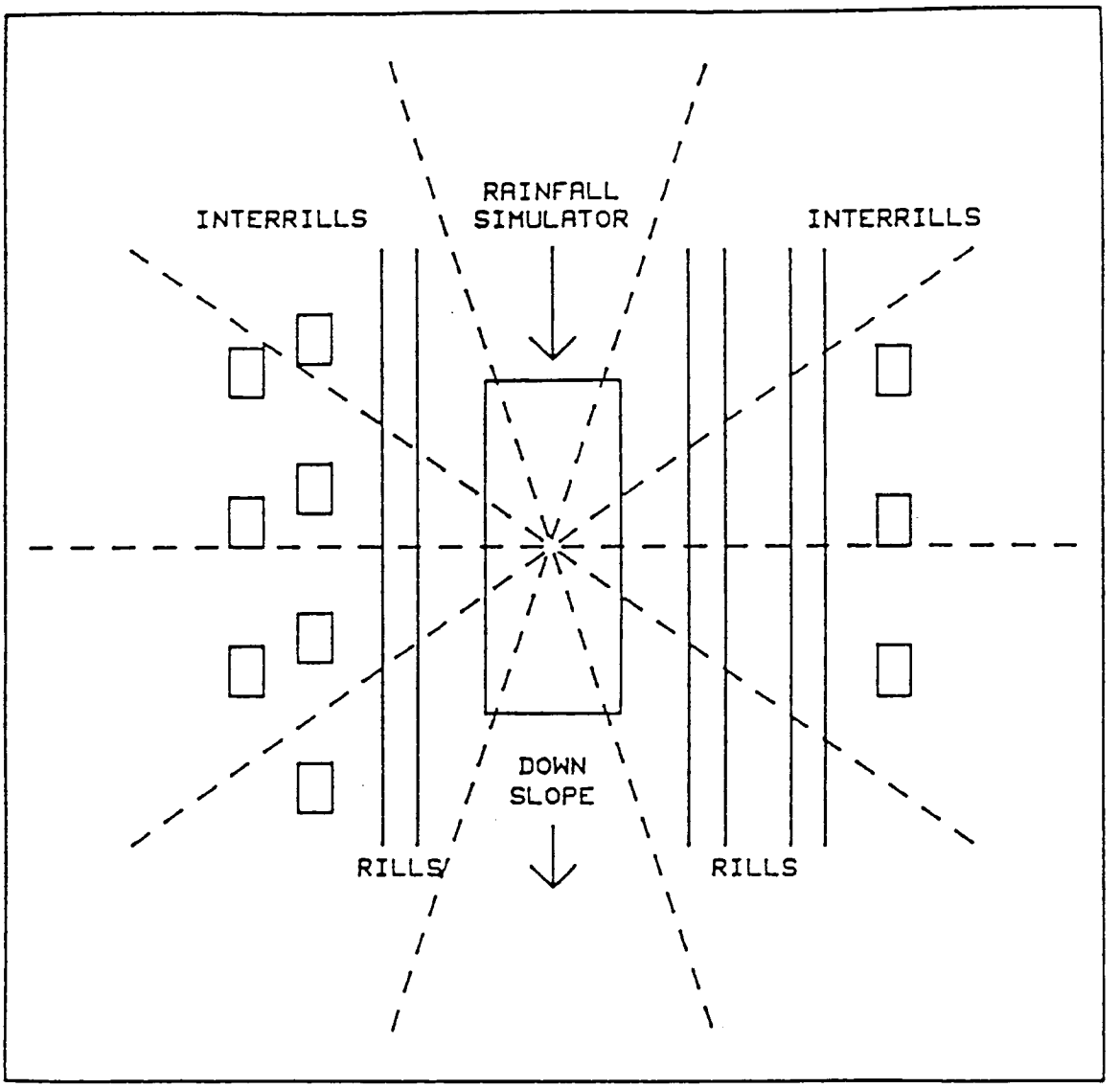

Figure 2. Typical plot arrangement for cropland rainfall simulator experiments. (from Laflen et al., 1987)

collected from rill and interrill plots to determine the runoff rates and sediment concentrations. Interrill plots were not sampled further. The next run consisted of rainfall application and addition of increasing rates of clear water at the top of each rill. Rainfall was applied at the same rate as before and inflow was started at 8 l/min and increased in 8 l/min increments up to 40 l/min. At each inflow level (including no inflow), velocity, runoff, and sediment concentration samples were taken when runoff reached equilibrium. In the last run, added inflow was introduced at the same rates as for the second run and samples taken but no rainfall was applied.

This procedure was designed to measure the soil erodibility parameters for rill and interrill areas (Laflen, et al. 1987). The interrill erodibility parameter K_i could be determined from the interrill plot data since all of the soil removed from the plot would be the result of raindrop detachment and thin sheet overland flow.

The addition of different levels of inflow to the rills was designed to simulate the effects of increasing hydraulic shear. From these data, it was proposed that the values of K_r and t_c could be found by simple linear regression with sediment discharge rate as a function of K_r, τ, and τ_c. Nearing et al. (unpublished manuscript) has pointed out that two assumptions are made for this method that do not correspond to field data or to the current erosion modeling technology. The first is that the rill detachment rate is not reduced by partial filling of the transport capacity of the flow. It is also assumed that flow shear stress in the rill does not increase in the downslope direction even though flow rate increases.

Rangelands

Rangeland sites usually consisted of six 3.05 x 10.7 m plots. Plots were treated one of three ways: natural, clipped (canopy clipped to about 2 cm and removed), or bare (vegetative canopy and surface cover removed). Two plots of each treatment were prepared at a site. In addition, two 0.6 x 1.2 m interrill plots were installed next each of to the large bare plots. These interrill plots were also bared and one of them was covered with window screening to dissipated raindrop energy.

The procedures for the simulator runs were described by Simanton et. al. (1987). Two adjacent plots with different treatments were run at the same time (Fig. 3). The simulation sequence for each plot pair consisted of a dry run (60 min at about 65 mm/hr) followed 24 hours later by a wet run (30 min at about 65 mm/hr) which was followed 30 minutes later by a very wet run. During the very wet run, the rainfall intensity rate started at about 65 mm/hr then was increased to about 130 mm/hr and decreased back to about 65 mm/hr. For the large bare plots, in the last phase of the run (about 65 mm/hr rainfall) overland flow was applied to the top of the plot at 3 or 4 rates corresponding to runoff rates varying from about 40 to 200 mm/hr. The length of time at each rainfall rate and overland flow application rate depended on the time to reach runoff equilibrium.

Sediment concentration samples were taken during each run at each level of rainfall and overland flow (where applied) on each plot. Runoff rate was continuously monitored with pressure transducer bubble gauges that recorded the water depth in the calibrated flumes installed at the outlet of the large plots. Runoff volumes and sediment amounts and volumes were determined from integration of the hydrograph and

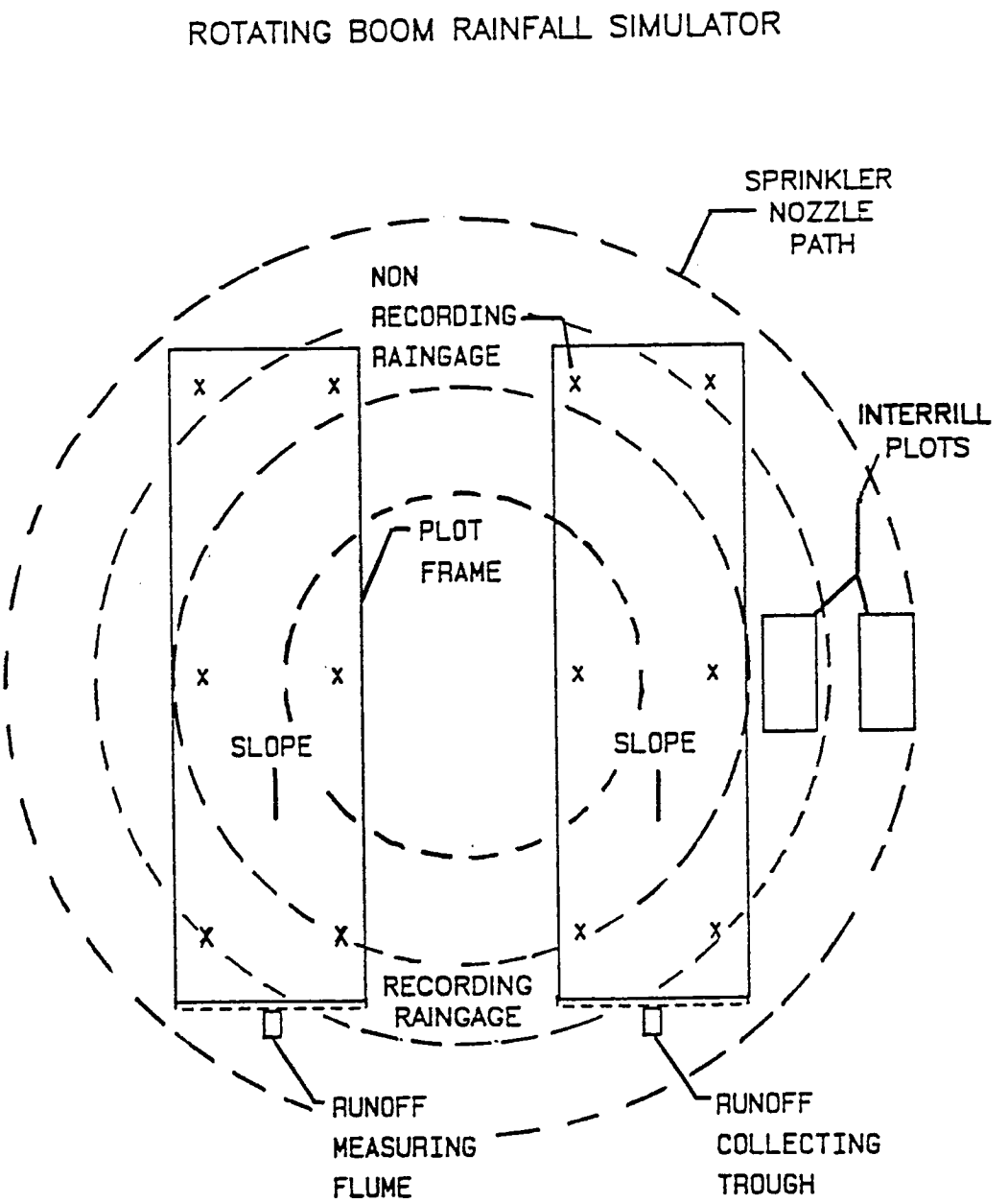

Figure 3. Typical plot arrangement for rangeland rainfall simulator experiments. (from Simanton et al., 1987).

sedigraphs. Interrill plots' runoff rates and volumes were determined from timed volumetric samples.

As with the cropland interrill plots, the rangeland interrill plots were designed to estimate K_i. The simulations on the large plots were not designed to test rill and interrill erodibility separately. Normal rangeland practices do not include soil tillage. Creation of preformed rills would result in unnatural conditions which could lead to parameter values that would not be applicable to normal rangeland conditions (Simanton, et al., 1987). The rill erodibility parameters must be based on assumptions of flow partitioning and channel hydraulics for the large plots.

Optimization

A method was needed to evaluate the erosion model parameters from the cropland and rangeland field data because of the problems described above in trying to directly solve for them. Blau et al. (1988) have shown that optimization techniques could be used to obtain erodibility parameters from field data for a physically based dynamic erosion model proposed by Shirley and Lane (1978) and described in detail by Lane et al. (1988). The advantages of this approach are that both cropland and rangeland parameter values could be found with the data available and computations could be made using the same relationships that are found in the WEPP erosion model. The WEPP model (Lane et al., 1987) is not the same model used by Blau et al. (1988).

In this optimization, values for the WEPP model erodibility parameters (K_i, K_r, and τ_c) are found with a least squares optimization routine described by Nearing et al. (unpublished manuscript). Measured sediment load data are input and predicted sediment loads using various

combinations of parameter values are found. The parameter values that are output are the ones that minimize the least squared differences between the measured and predicted sediment loads. Testing of this procedure has shown that there are no apparent problems in the use of it to obtain parameter estimates (Nearing et al. unpublished manuscript).

Data Used in Analyses

One of the objectives of this study was to evaluate the effect on the erodibility parameters of calculating rill shear stress from overland sheet flow compared with flow partitioned into rills. The erodibility parameters for these two cases were found by running the optimization program with different versions of the erosion model.

The optimization program was run with data from four cropland soils and five rangeland soils. Information on the soils is shown in Tables 1 and 2. The model inputs included measured rainfall intensities, runoff discharge rates and sediment loads for both croplands and rangelands. In addition, for croplands, measured flow velocities in the rills were input to be used to calculate rill friction factors. Rill flow velocities were not measured on rangeland plots so a friction factor of 1.7 was used for calculations. This has been determined to be a reasonable value for some rangeland plots (Nearing, unpublished WEPP model documentation). The space between rills was 0.48 m for croplands and estimated as 1 m for rangelands.

The input data used is presented in Appendix A. There were 6 sets of data for each cropland soil (one for each bare rill) and 2 sets for each rangeland soil (one for each large plot). The four versions of the 3-parameter optimization that were run were:

Table 1. Soil texture and slope information for the four cropland sites.

SITE	SOIL	PLOT	SAND %	SILT %	CLAY %	ORGANIC MATTER %	SLOPE
Lincoln, NE	Sharpsburg	1	3.7	55.7	40.6	1.85	0.059
		2					0.059
		3					0.059
		4					0.059
		5					0.053
		6					0.053
Big Spring, TX	Amarillo	1	84.4	9.8	5.8	0.16	0.034
		2					0.034
		3					0.034
		4					0.034
		5					0.032
		6					0.032
Waco, TX	Heiden	1	8.6	38.3	53.1	1.36	0.033
		2					0.033
		3					0.033
		4					0.033
		5					0.034
		6					0.034
Pullman, WA	Walla Walla	1	15.3	74.2	10.5	1.49	0.075
		2					0.065
		3					0.059
		4					0.064
		5					0.056
		6					0.048

Table 2. Soil texture, slope, and ground cover information for the five rangeland sites.

SITE	SOIL	PLOT	SAND %	SILT %	CLAY %	ORGANIC MATTER %	SLOPE %	GROUND COVER %
Chickasha, OK	Grant	72	53.8	31.8	14.4	1.9	0.05	7.6
		74						14.1
Woodward, OK	Pratt	85	88.0	8.7	3.3	0.6	0.15	8.2
		89						7.1
Meeker, CO	Degater	108	6.5	49.3	44.2	1.4	0.10	13.7
		110						12.4
Cottonwood, SD	Pierre	114	14.4	44.5	41.1	2.5	0.08	27.3
		116						29.8
Cuba, NM	Querencia	131	66.5	24.3	9.2	0.8	0.08	26.4
		134						31.8

1. cropland sheet flow
2. cropland rill flow
3. rangeland sheet flow
4. rangeland rill flow.

In addition, the optimization could be run for 2 parameters, K_r and τ_c, when an estimate of K_i was available. Since K_i could be estimated from the interrill plot data for both cropland and rangeland soils, two parameter optimizations were run for the four cases described above. This allowed for the comparison of parameter values and sediment loads from the 2- and 3-parameter optimizations to see if there was any advantage of using one over the other.

CHAPTER 4

RESULTS

Shear Stress on a Uniform Plane

Uniform sheet flow assumes that the depth of flow on a plane does not vary in space. Shear stress estimated from sheet flow is based on the depth of the water. When the same amount of water concentrates in a rill, the shear stress increases because the water depth increases. The sides of the rill also become a factor in the resistance to flow. Examples of the magnitude of the difference in shear stress based on these two conditions is shown in Figures 4 and 5.

Figure 4 shows the shear stresses along a 1 x 100-m plane with 9 percent slope and a 10-cm deep triangular rill. These results were computed for a rainfall excess rate of 50 mm/hr and assumed that all of the runoff flowed into the rill. Rill flows ranged from .14 to 14 * 10^{-4} m^2/s. Shear stress is plotted for 7 different rill widths for each of the first 10 m downslope and for 10 m increments after that. Shear stresses for two pairs of rills (10 and 40 cm, 5 and 80 cm) were the same because each pair had the same hydraulic radius. The shear stress from rill flow (τ_r) is shown to be greater than from sheet flow (τ_s). For example, for typical rill widths of 5, 10, and 20 cm, τ_r is 2.9, 3.6, and 3.9 N/m^2 (respectively) times greater than τ_s at 50 m downslope. This difference is even larger near the top of the plane with τ_r about 8 to 11 times greater than τ_s at 1 m downslope.

Figure 5 shows τ_r and τ_s for a 10-cm deep rectangular rill plotted for the same conditions as the triangular rill. It also shows τ_r values greater than τ_s, especially at the narrower rill widths. As the width increases in a rectangular rill the flow becomes closer to sheet flow so

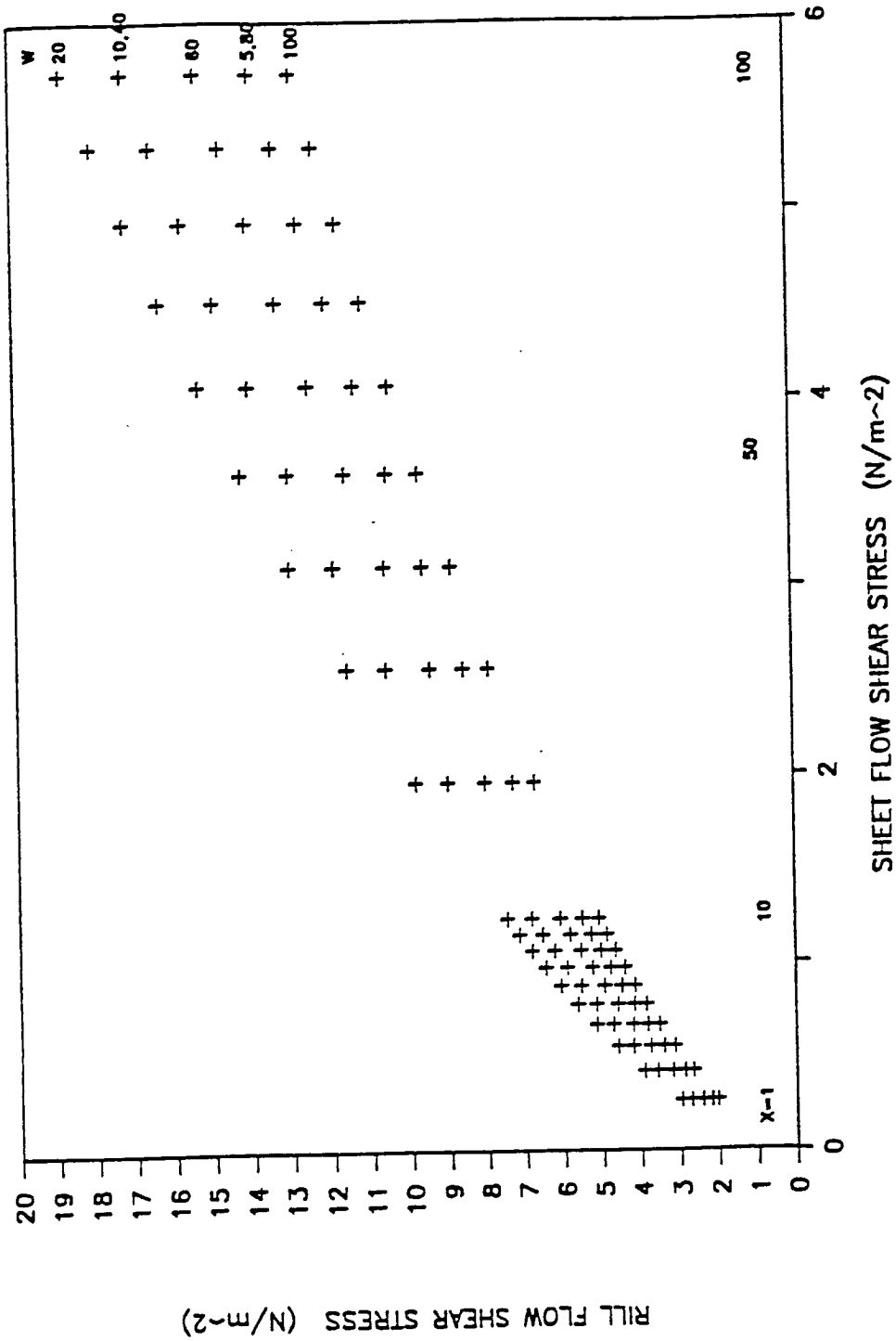

Figure 4. Comparison of shear stress calculated from rill and sheet flow for a 10 cm deep triangular rill. Values shown are for various distances (X) down a 9%, 100-m slope for 7 rill widths (W).

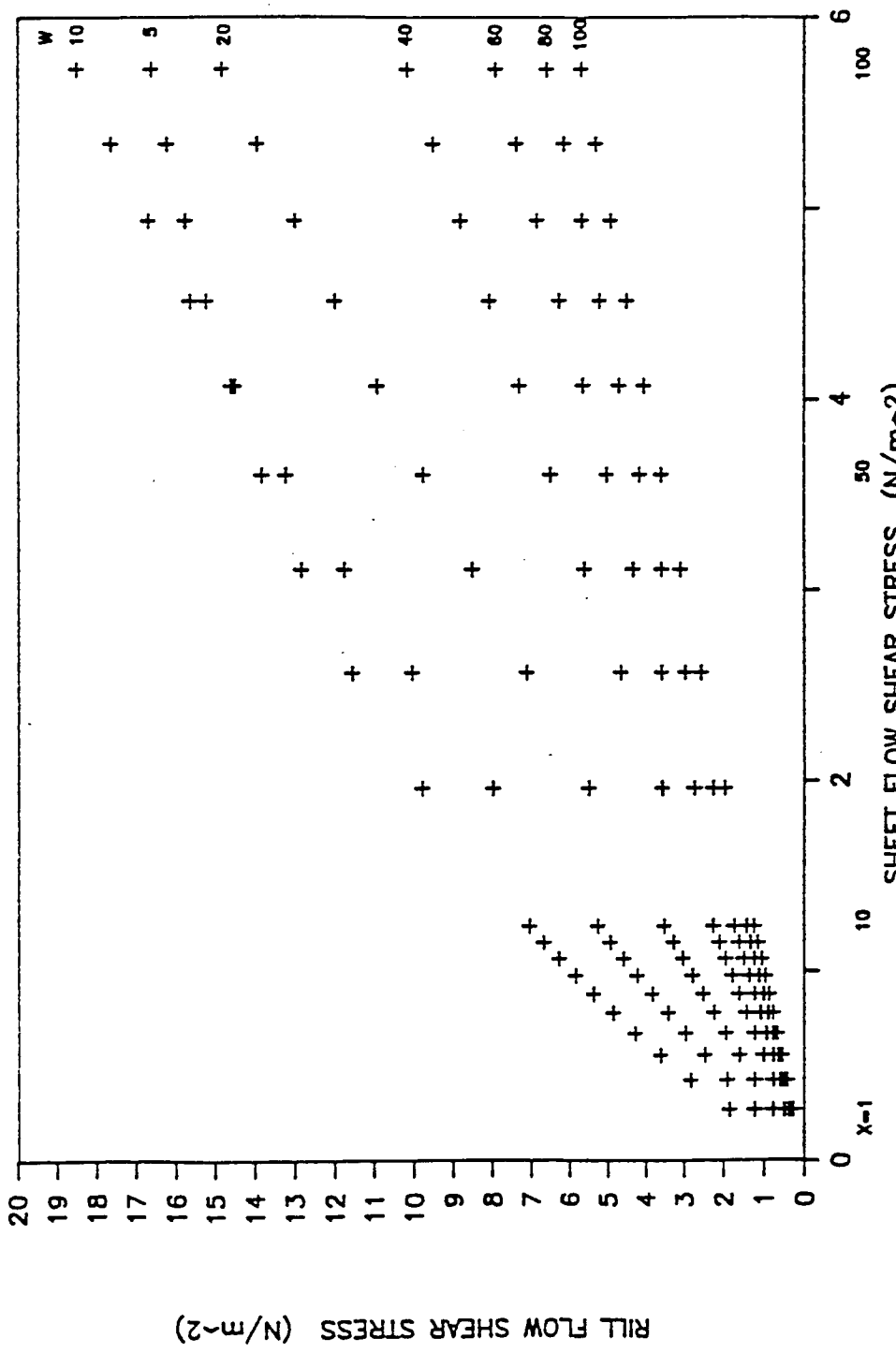

Figure 5. Comparison of shear stress calculated from rill and sheet flow for a 10 cm deep rectangular rill. Values shown are for various distances (X) down a 9%, 100-m slope for 7 rill widths (W).

that the 100 cm rill (on a 1-m wide plane) represents sheet flow and has τ_r values equal to τ_s.

These results help point out the importance of using τ_r for rills. For each set of conditions, there is a threshold shear stress associated with detachment (τ_c). Rill erosion can begin when the shear stress exceeds the τ_c. For the case of a 5 cm wide rectangular rill with a τ_c of 5 N/m^2, if τ_s is assumed, then rilling would be predicted to start about 80 m downslope. If τ_r is assumed, rilling would be predicted between 5 and 6 m downslope. Since τ_r is a better estimate of the rill shear stress, rilling would more likely start near the top of the slope. Figure 6 shows that for a rectangular channel, the distance to rilling increases linearly (r^2=.996) with rill width.

The rill geometry that is assumed for an erosion model is important in the calculation of the hydraulics of the flow. Triangular and rectangular geometries were the two fairly simple possibilities tested here. The results show similar τ_r values for the narrower rills (5, 10, and 20 cm) which are close to the rill widths found in the field. The triangular rill was an attractive candidate because the flow depth could be solved for analytically but the rectangular geometry was chosen for the model because it was felt that it more accurately represented the geometry of rills observed in the field. The rectangular geometry was also the basis of the width-discharge relationship (Equation 19) used in CREAMS (Lane and Foster, 1980a).

Effect of Rill Spacing and Rill Width

The distance between rills (rill spacing) and the rill width both affect the shear stress of flow in rills and lead to changes in the sediment load of the flow. The effects of changing the rill spacing and

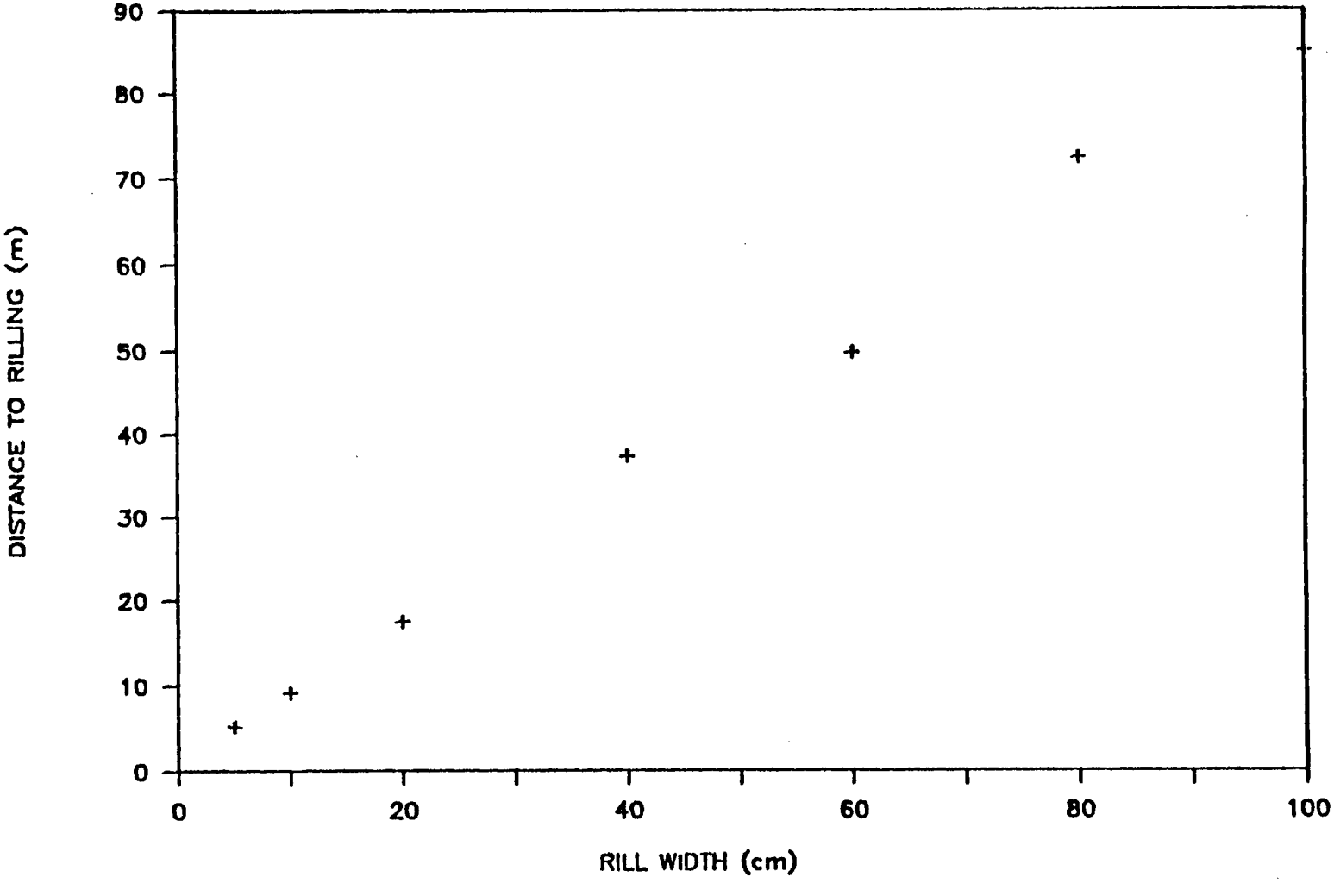

Figure 6. Estimated distance to the start of rill erosion for different widths of a rectangular rill on a 100-m, 9% slope with τ_c =5.0 N/m^2.

the rill width on the sediment loads predicted with the WEPP erosion model for 3 different values of τ_c are shown in Figures 7 and 8.

Figure 7a shows that at low τ_c (1.0 N/m^2) there was a slight increase in the predicted sediment load as rill spacing increases from 0.5 to 2.0 m. This increase was 10.5% and 8.5% for the low (60 mm/hr) and high rainfall intensities (120 mm/hr) respectively. Figure 7b shows that at higher τ_c (5.0 N/m^2), the predicted sediment loads increase 67% for the lower rainfall intensity and 37% for the higher intensity as the distance between rills increases from 0.5 to 2.0 m. Figure 7c shows that for a high τ_c (10.0 N/m^2), at the low rainfall intensity, there is very little increase in sediment load (5.0%) between the 0.5 and 2.0 m rill spacing. For the higher intensity, sediment loads are about the same for the first two rill spacings then increase as the rills get farther apart.

For all 3 values of τ_c (Fig. 7), predicted sediment loads at each rainfall intensity increase for increasing K_i values. The relationship between the sediment loads for different values of K_i at each rill spacing stayed about the same. This indicates that sediment loads the for different K_i values are not affected by the distance between rills, as expected, since rill spacing affects the rill detachment while K_i mainly affects the interrill detachment.

The effect of increased distance between rills is to route more flow into each rill. This leads to increased depth of flow and shear stress and, depending on τ_c, increased sediment loads. At low τ_c values, even low flows will have enough shear stress to exceed τ_c and cause detachment so increasing the rill spacing will not cause sharp increases in predicted sediment loads. At moderate values of τ_c (5 N/m^2) and

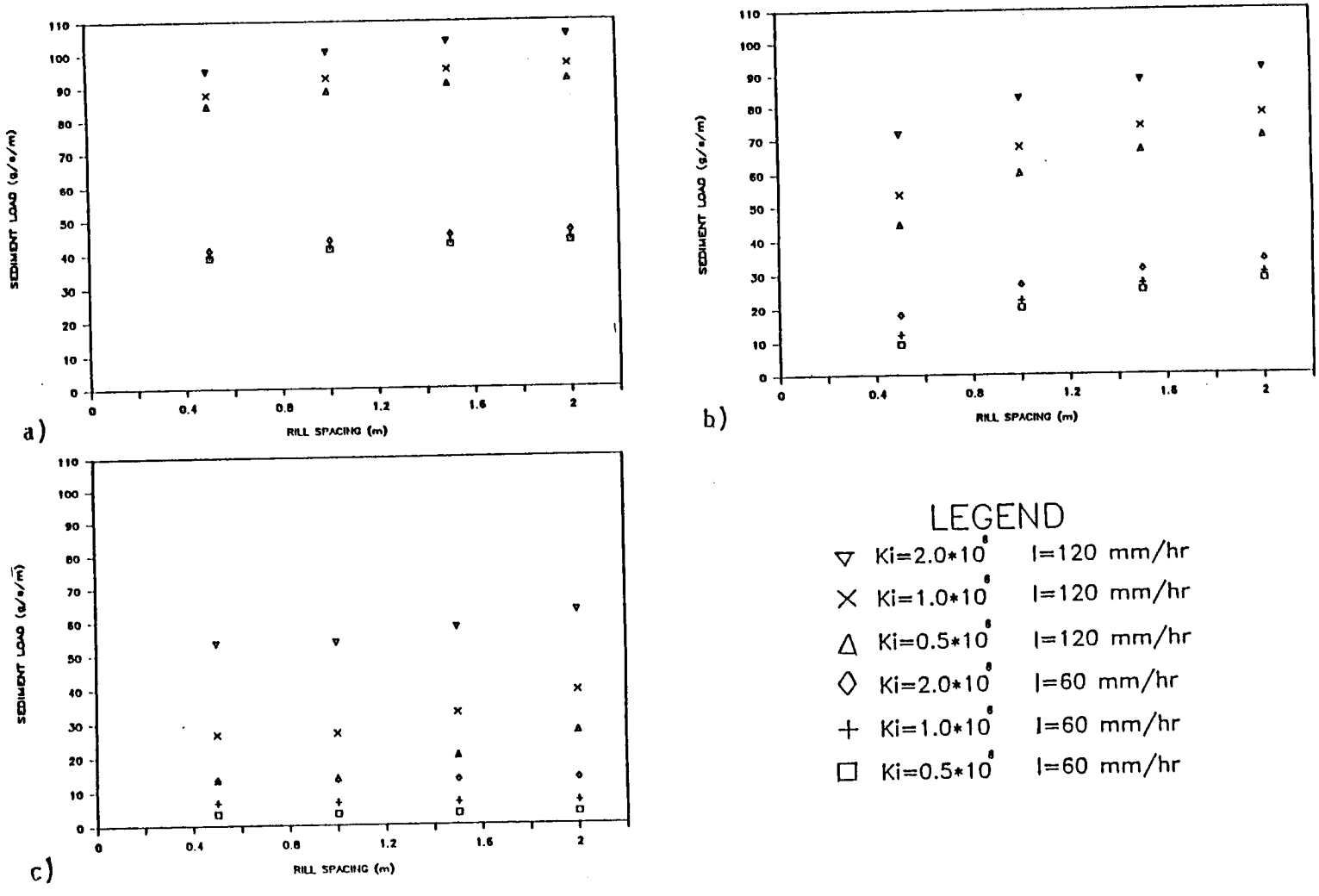

Figure 7. The effect of rill spacing on sediment load for 2 rainfall intensities (I) and 3 K_i values for a) τ_c=1.0 N/m^2 b) τ_c=5.0 N/m^2 and c) τ_c=10.0 N/m^2. K_i units are kg*s/m^4.

small rill spacings, the shear stress of the flow may not exceed τ_c so there is no flow detachment. As rill spacing increases, the increased rill flow reaches a point where its' shear stress is greater than τ_c and flow detachment causes a large increase in sediment load. When τ_c is high (10 N/m^2), the flow in the rill must be very large to have a shear stress high enough to cause detachment. In this study, this only occurred at the two highest rill spacings for the highest rainfall intensity.

The effects of changing rill width on predicted sediment loads are shown in Figure 8. Rill widths were increased by increasing the value of the coefficient (a) in the equation for calculating width (Equation 19).

At low τ_c (1.0 N/m^2), sediment loads increased 50-60% with a fourfold increase in rill width (Fig 8a) for each rainfall intensity. Figure 8b shows that at a higher τ_c (5 N/m^2) sediment loads reached a maximum then began to decrease as rill width increased. When τ_c was high (10 N/m^2) increased rill width had little or no effect on the predicted sediment loads. There was only a slight decrease in sediment load for the two narrowest rills at the high rainfall intensity.

Predicted sediment loads at each rainfall intensity increased as K_i values increased for all 3 values of τ_c (Fig. 8). The relationship between the sediment loads for different K_i values stayed the same. As noted in the rill spacing study, this is expected since rill width affects only rill detachment.

Rill width can affect sediment load in two ways. Increased rill width decreases the depth of flow and usually leads to lower shear

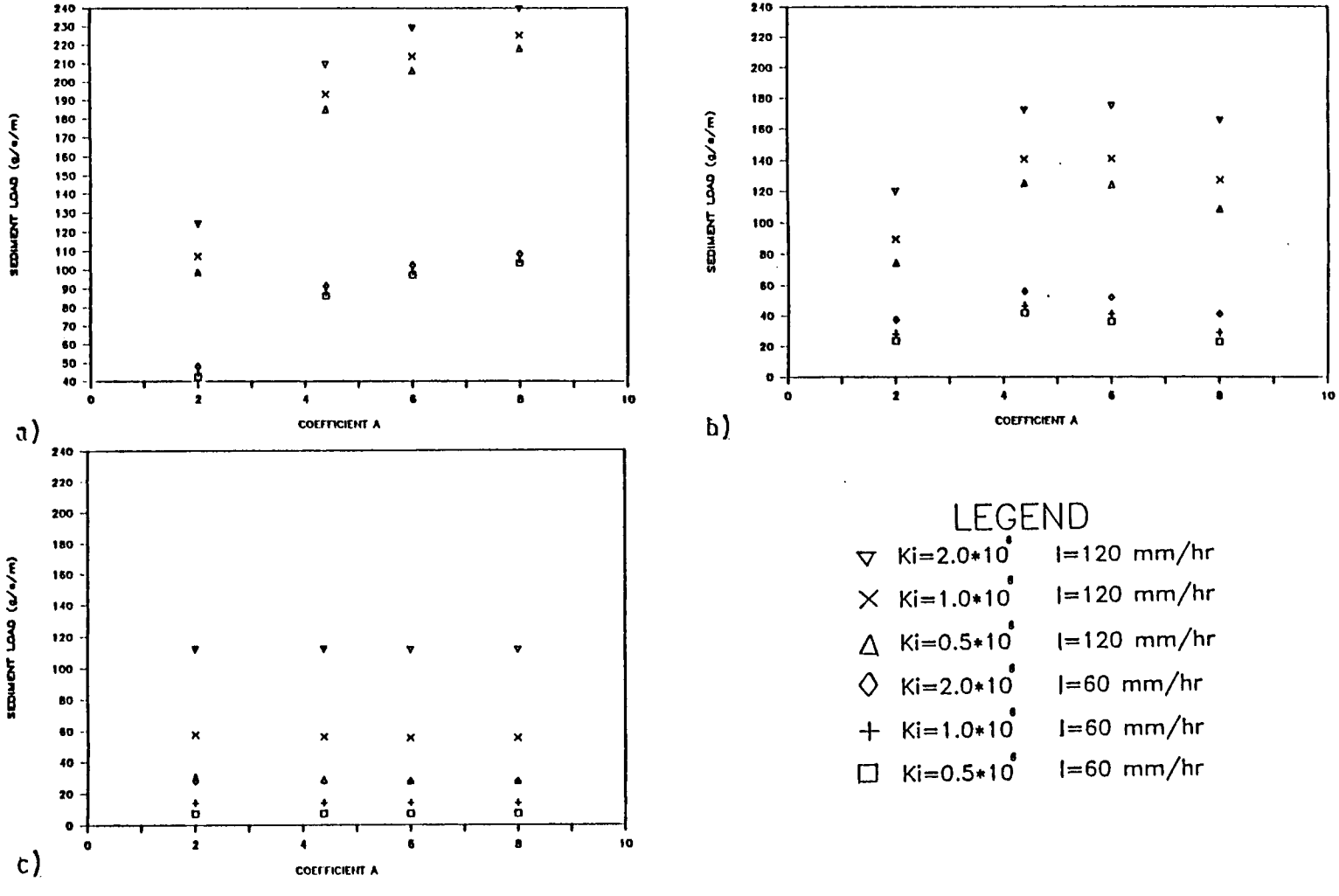

Figure 8. The effect of rill width on sediment load for 2 rainfall intensities (I) and 3 K_i values for a) τ_c=1.0 N/m^2 b) τ_c=5.0 N/m^2 and c) τ_c=10.0 N/m^2. K_i units are kg*s/m^4.

stress in a rectangular rill which would tend to decrease detachment. At the same time, the flow is spread over a wider area could therefore increase detachment. The observed effect on sediment load is caused by the interaction of these two opposing forces.

For the conditions studied, at low τ_c, where the shear stress of the flows were larger than τ_c, as rill width increased, the increased area available to erode had more of an effect than the lower shear stress and led to larger sediment loads in all cases. At moderate τ_c values, as rill width increased, sediment loads increased to a maximum then the effect of reduced shear stress became more important than the increased detachment area and sediment loads decreased. For high τ_c values, the shear stress of most of the flows was not high enough to exceed τ_c so the increased rill width had no effect.

Optimization

The erodibility parameter values (K_i, K_r, and τ_c) and predicted sediment loads for two versions of the WEPP erosion model were found using optimization techniques. One version estimated shear stress based on an assumption of sheet flow (τ_s) while the other used width and flow depth estimates (Equation 19 and Fig. 1) of the rill flow to calculate shear stress (τ_r). Parameter values and sediment loads were estimated from field data for four cropland and five rangeland soils.

In addition, the experimental design of both cropland and rangeland tests allowed for the estimation of the interrill erodibility parameter, K_i, for each site. The effect of the field estimated K_i on the other parameters and on the optimized sediment loads was investigated using a 2-parameter optimization (for K_r and τ_c). These parameter values and

sediment loads were compared to results from the 3-parameter optimization.

Cropland and rangeland experimental methods differed because of the inherent nature of two types of areas. The results of the optimized sediment loads and parameter values will be discussed separately for cropland and rangeland sites. Results are based on data for 10 rangeland plots from 5 sites and 22 cropland rills from 4 sites. Two cropland rills (Amarillo rill 3 and Heiden rill 6) were not included because of probable errors in the field data.

Comparison of Measured and Optimized Sediment Loads

The ability of the optimization to predict sediment loads that closely match measured values is important in determining if optimization is an appropriate method of estimating parameter values. Large differences in the measured and optimized values could indicate problems with the field data or the optimization.

Croplands

The optimized sediment loads for the τ_r (partitioned rill flow) and τ_s (sheet flow) assumptions were both close to the measured values (Figs. 9-12 and Appendix B). The values of the least squared objective function (LS) were similar for τ_r and τ_s in most cases for individual rills (Tables 3 and 5) and the mean LS values were similar for a site (Tables 4 and 6). Large LS values were often the result of the magnitude of the sediment load used in the optimization. The r^2 for the measured and optimized values (Table 7) was very high for all soils for both the τ_r and τ_s cases. This suggests that sediment load can be estimated equally well from τ_r and τ_s assumptions.

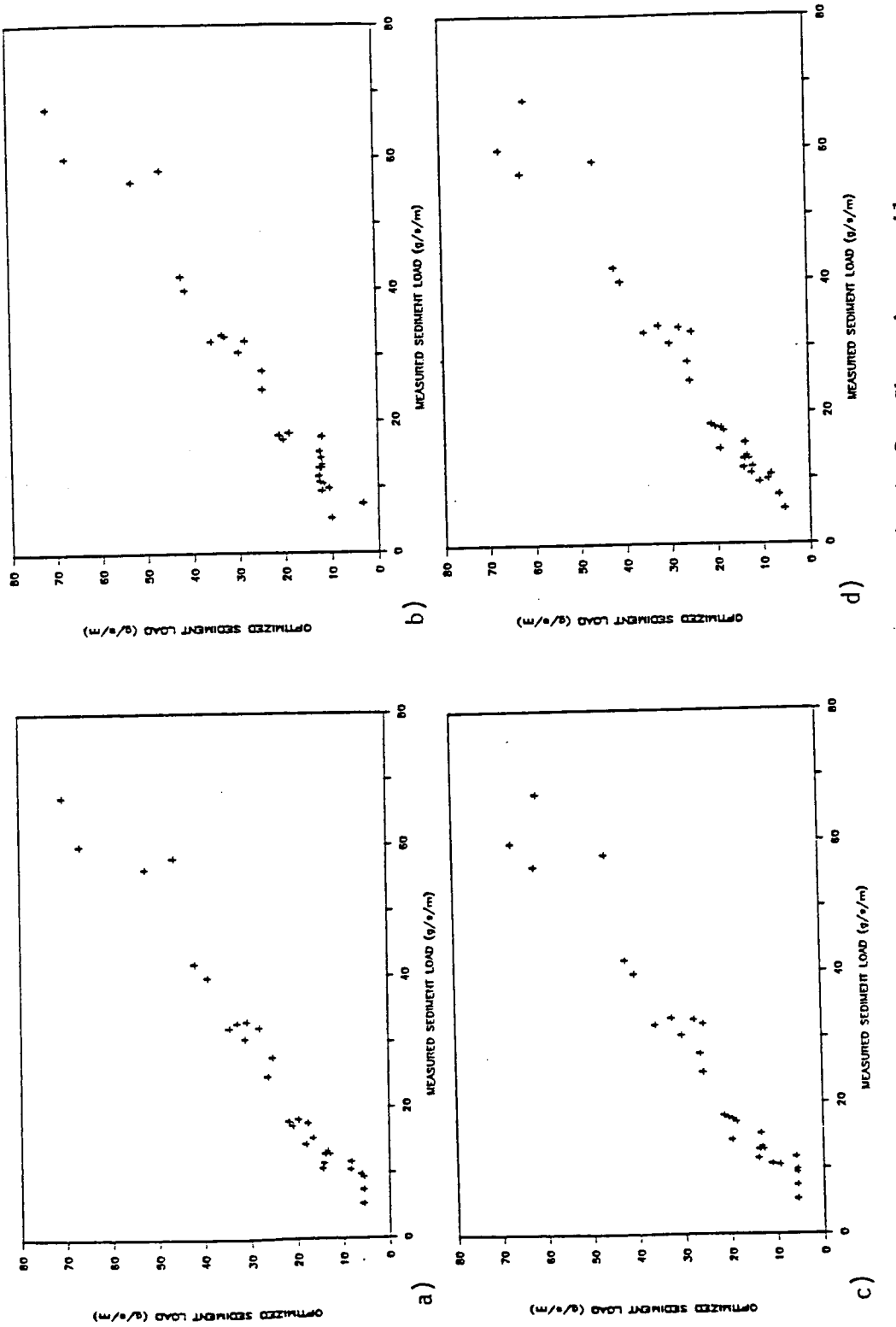

Figure 9. Measured and optimized sediment loads for Sharpsburg soil. Optimized values based on a) 2-parameter r_s b) 3-parameter r_s c) 2-parameter r_r and d) 3-parameter r_r calculations.

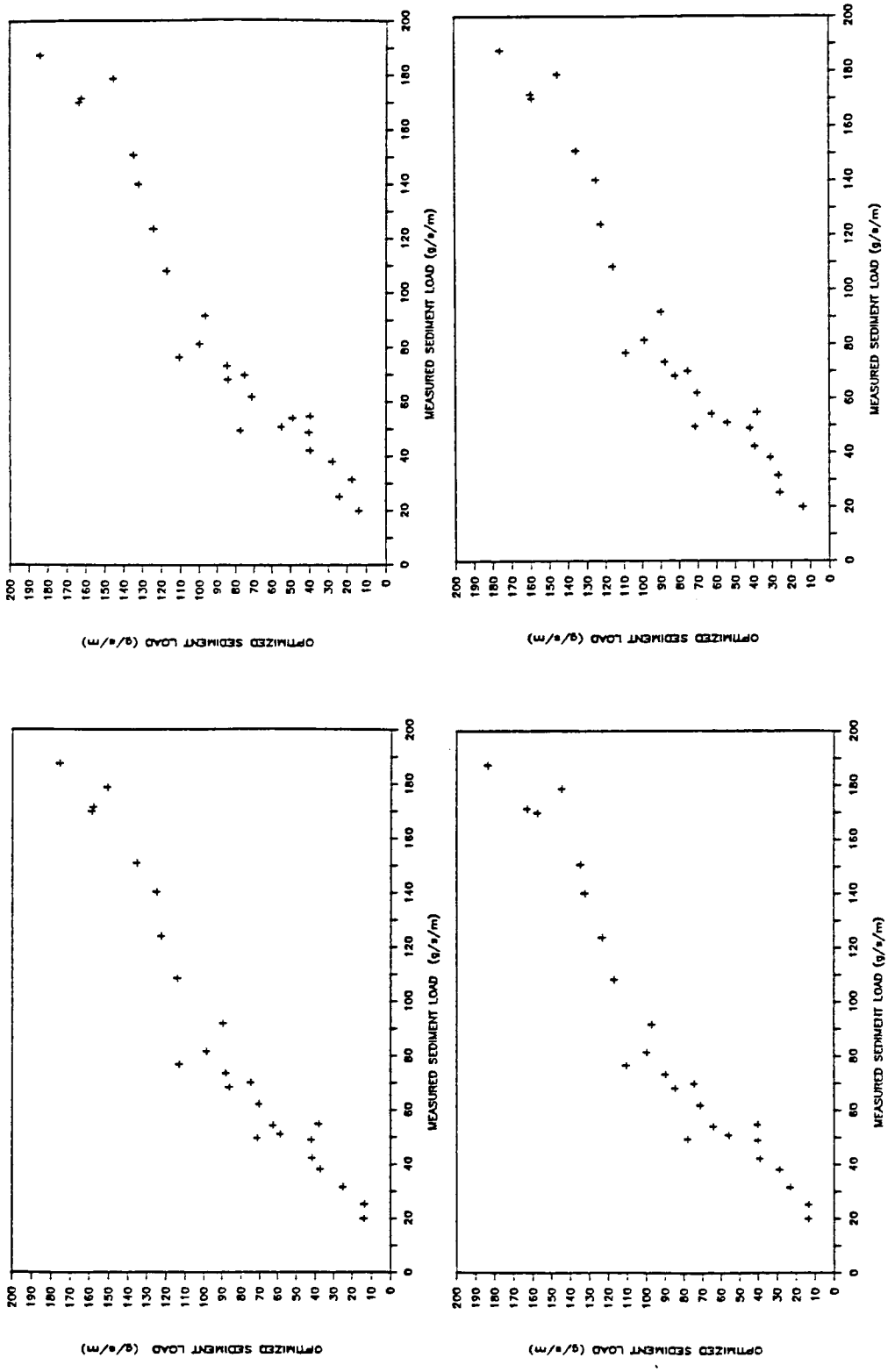

Figure 10. Measured and optimized sediment loads for Amarillo soil. Optimized values based on a) 2-parameter τ_c b) 3-parameter τ_s c) 2-parameter τ_r and d) 3-parameter τ_r calculations.

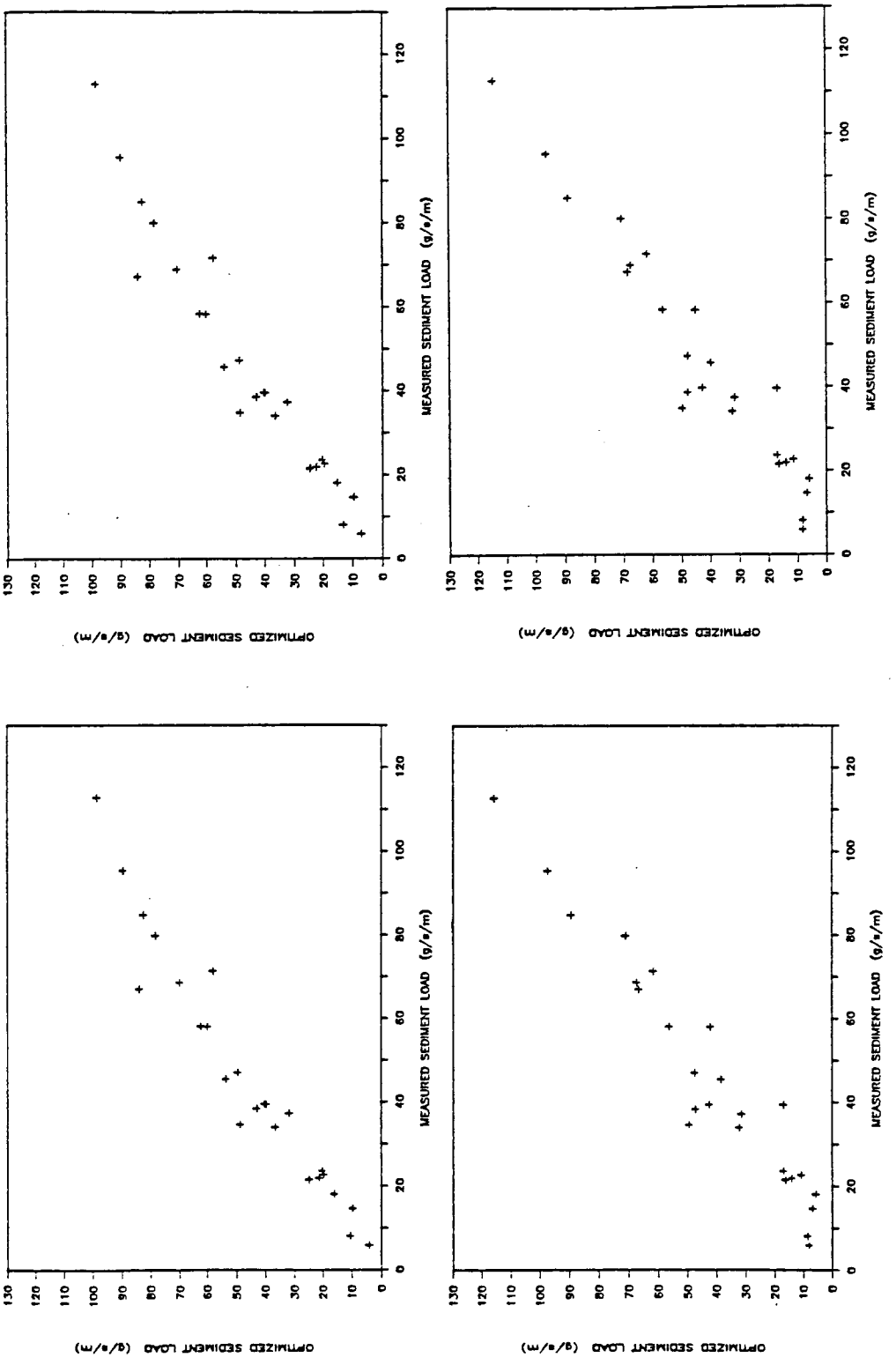

Figure 11. Measured and optimized sediment loads for Heiden soil. Optimized values based on a) 2-parameter τ_s b) 3-parameter τ_s c) 2-parameter τ_r and d) 3-parameter τ_r calculations.

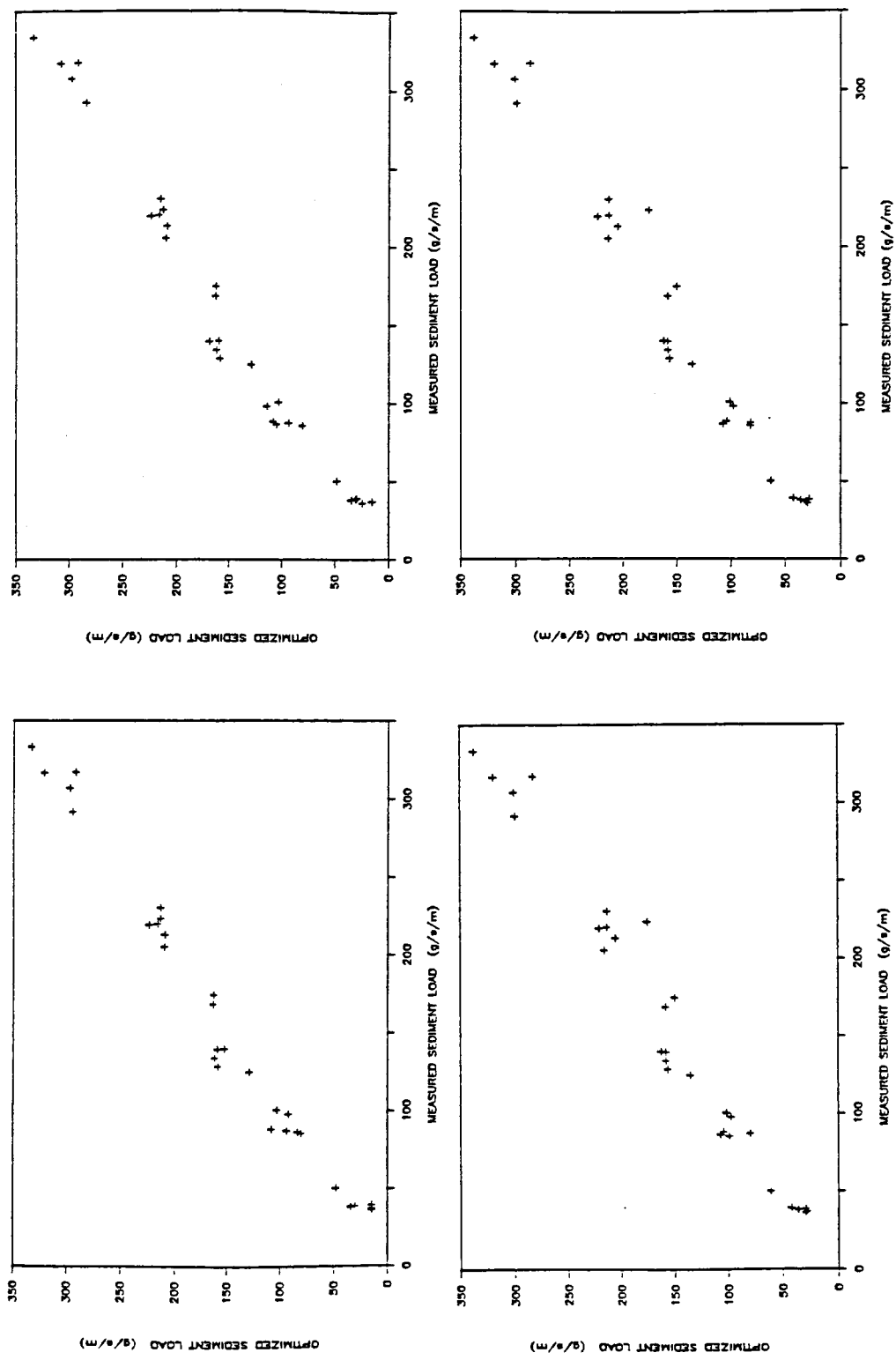

Figure 12. Measured and optimized sediment loads for Walla Walla soil. Optimized values based on a) 2-parameter r_r b) 3-parameter r_s c) 2-parameter r_r and d) 3-parameter r_r calculations.

Table 3. Cropland parameter and least square (LS) values for rill flow (R) and sheet flow (S) shear stress estimations for the 2-parameter optimization.

SOIL	RILL	K_i R	K_i S	K_r R	K_r S	τ_c R	τ_c S	LS R	LS S
		$* 10^{-6}$	$* 10^{-6}$	$* 10^{3}$	$* 10^{3}$				
		$kg\text{-}s/m^4$	$kg\text{-}s/m^4$	s/m	s/m	N/m^2	N/m^2		
Sharpsburg	1	1.98	1.98	4.28	1.33	5.782	1.457	81.88	44.95
	2	1.98	1.98	2.75	1.37	1.996	1.226	61.87	19.02
	3	1.98	1.98	8.56	2.87	5.309	1.934	82.41	50.68
	4	1.98	1.98	6.91	2.73	3.066	1.547	196.87	198.26
	5	1.98	1.98	5.10	1.18	5.617	0.988	40.32	34.91
	6	1.98	1.98	5.93	1.84	6.173	1.638	15.37	15.35
Amarillo	1	4.50	4.50	65.02	14.65	4.259	1.111	454.22	589.69
	2	4.50	4.50	47.57	12.67	4.856	1.420	698.31	798.43
	4	4.50	4.50	62.72	18.27	0.000	0.741	1148.94	1123.34
	5	4.50	4.50	119.01	22.72	5.041	1.461	381.32	313.86
	6	4.50	4.50	67.49	14.16	0.000	0.988	2514.60	2703.41
Heiden	1	1.44	1.44	19.75	6.58	0.000	0.720	919.65	490.24
	2	1.44	1.44	14.16	3.29	0.844	0.967	404.35	422.75
	3	1.44	1.44	22.39	7.74	0.000	1.296	105.47	114.96
	4	1.44	1.44	31.11	2.47	0.885	0.782	103.32	41.93
	5	1.44	1.44	11.03	5.10	0.000	0.761	322.91	54.91
Walla Walla	1	4.26	4.26	20.08	12.02	2.469	1.996	689.11	1210.75
	2	4.26	4.26	25.35	10.37	3.992	1.255	752.49	948.54
	3	4.26	4.26	43.46	17.94	4.774	1.872	3307.67	885.05
	4	4.26	4.26	14.32	7.74	0.309	1.111	991.31	230.88
	5	4.26	4.26	131.69	42.63	5.864	2.099	2201.60	2085.60
	6	4.26	4.26	85.76	20.91	5.082	1.235	435.72	453.26

Table 4. Statistics for the cropland parameter and least square values for the 2-parameter optimization. STD=standard deviation, CV=coefficient of variation R=rill flow and S=sheet flow shear stress estimations.

SOIL	STAT	K_r R $* 10^3$ s/m	K_r S $* 10^3$ s/m	τ_c R N/m^2	τ_c S N/m^2	LS R	LS S
Sharpsburg	MEAN	5.59	1.89	4.66	1.47	79.79	60.53
	STD	2.03	0.74	1.70	0.33	62.84	68.89
	CV	0.36	0.39	0.37	0.22	0.79	1.14
Amarillo	MEAN	72.36	16.49	2.83	1.14	1039.48	1105.74
	STD	27.21	4.04	2.60	0.30	877.50	940.84
	CV	0.38	0.25	0.92	0.26	0.84	0.85
Heiden	MEAN	19.69	5.04	0.35	0.91	371.14	224.96
	STD	7.80	2.20	0.47	0.24	334.14	214.48
	CV	0.40	0.44	1.37	0.26	0.90	0.95
Walla Walla	MEAN	53.44	18.60	3.75	1.59	1396.32	969.01
	STD	46.26	12.75	2.04	0.44	1122.78	651.69
	CV	0.87	0.69	0.54	0.28	0.80	0.67

Table 5. Cropland parameter and least square (LS) values for rill flow (R) and sheet flow (S) shear stress estimations for the 3-parameter optimization.

SOIL	RILL	K_i R * 10^{-6} kg-s/m^4	K_i S * 10^{-6} kg-s/m^4	K_r R * 10^{3} s/m	K_r S * 10^{3} s/m	τ_c R N/m^2	τ_c S N/m^2	LS R	LS S
Sharpsburg	1	3.210	3.790	4.44	1.48	6.543	1.955	67.50	28.47
	2	0.481	4.210	2.52	1.98	0.000	2.181	54.64	40.99
	3	2.383	1.160	8.72	2.96	5.473	1.893	81.62	66.28
	4	1.951	3.568	6.91	2.80	3.066	1.749	196.85	219.70
	5	4.383	4.494	5.76	2.30	6.914	2.243	7.45	11.91
	6	3.868	4.346	6.26	2.14	6.996	2.222	2.08	10.70
Amarillo	1	0.004	5.827	68.31	19.75	3.868	1.502	415.16	392.10
	2	4.543	4.605	47.90	12.67	4.877	1.420	697.16	795.20
	4	4.403	2.852	64.03	18.64	0.000	0.679	1148.69	1105.46
	5	8.694	8.068	116.07	21.17	5.228	1.509	232.60	195.15
	6	0.004	1.062	73.09	15.14	3.395	0.905	2421.97	2624.95
Heiden	1	5.049	3.531	16.79	6.58	0.000	0.864	826.27	496.00
	2	1.267	0.350	13.50	3.29	0.576	0.864	404.57	419.93
	3	4.551	2.457	21.89	7.74	1.070	1.337	84.76	115.74
	4	2.436	4.247	36.87	2.30	1.667	1.070	102.52	54.13
	5	3.272	1.432	11.36	5.10	0.802	0.761	318.56	54.88
Walla Walla	1	4.654	1.840	20.08	9.38	2.531	1.173	686.04	1563.18
	2	1.741	4.102	24.53	10.37	3.358	1.235	751.42	946.63
	3	0.004	3.679	40.49	13.66	3.807	1.276	3207.20	1017.98
	4	5.593	0.070	13.42	7.74	0.000	0.844	979.42	227.26
	5	9.432	4.543	87.74	42.30	6.831	2.099	1781.18	2047.38
	6	2.531	3.679	87.74	20.91	4.959	1.214	434.07	445.95

Table 6. Statistics for the cropland parameter and least square values for the 3-parameter optimization. STD=standard deviation, CV=coefficient of variation R=rill flow and S=sheet flow shear stress estimations.

SOIL	STAT	K_i R	K_i S	K_r R	K_r S	τ_c R	τ_c S	LS R	LS S
		$*10^{-6}$	$*10^{-6}$	$* 10^3$	$* 10^3$				
		$kg\text{-}s/m^4$		s/m	s/m	N/m^2	N/m^2		
Sharpsburg	MEAN	2.71	3.59	5.77	2.28	4.83	2.04	68.35	63.01
	STD	1.42	1.24	2.12	0.54	2.79	0.20	70.68	79.48
	CV	0.52	0.35	0.37	0.24	0.58	0.10	1.03	1.26
Amarillo	MEAN	3.53	4.48	73.88	17.47	3.47	1.19	983.12	1022.57
	STD	3.65	2.69	25.41	3.48	2.08	0.38	75.40	962.85
	CV	1.03	0.60	0.34	0.20	0.60	0.32	0.89	0.94
Heiden	MEAN	3.32	2.40	20.08	5.00	0.82	0.98	347.34	228.13
	STD	1.54	1.57	10.19	2.25	0.61	0.23	300.98	213.00
	CV	0.46	0.65	0.51	0.45	0.75	0.23	0.87	0.93
Walla Walla	MEAN	3.99	2.99	45.67	17.39	3.58	1.31	1306.55	1041.40
	STD	3.34	1.70	33.79	13.06	2.30	0.42	1039.15	679.88
	CV	0.84	0.57	0.74	0.75	0.64	0.32	0.80	0.65

Table 7. Cropland regression analysis results (r^2 values) of optimized vs. measured sediment loads.

SOIL	2 PARAMETER		3 PARAMETER	
	RILL	SHEET	RILL	SHEET
Sharpsburg	0.947	0.959	0.953	0.957
Amarillo	0.922	0.915	0.937	0.921
Heiden	0.933	0.941	0.935	0.940
Walla Walla	0.968	0.978	0.970	0.976

The 2 and 3-parameter optimizations both performed very well in predicting sediment load. The LS values were very close for the 2 and 3-parameter models for both τ_r and τ_s cases. The values of r^2 for measured and optimized values were high for all soils (Table 7) and there was little if any improvement in the 3-parameter optimization over the 2-parameter for the τ_r and the τ_s estimates.

The reasons for the lack of improvement in the 3-parameter results are related to the experiments and to the optimization. The experiments were performed in rills where the interrill contribution to the sediment load might be expected to be small compared to the rill. Calculation of interrill erosion rates using field estimated K_i values indicate that at the highest inflow level, interrill erosion accounted for an average of about 8% of the total erosion. The optimization finds the least squares difference between measured and optimized values so the high inflow levels which have the highest sediment loads are the ones that are most important for the optimization to fit closely. Fixing the K_i value to a reasonable value would not affect the optimization much since interrill contribution at the highest inflow levels was low.

These results show that the optimized sediment loads from the 2-parameter optimization are very close to those predicted from the 3-parameter. Use of the 2-parameter optimization for these particular data would be reasonable since the rill experiments are not sensitive to K_i.

Rangelands

Optimized sediment loads were very close to the measured values for both the τ_r and τ_s cases (Figs. 13-17) except for the 2-parameter Grant

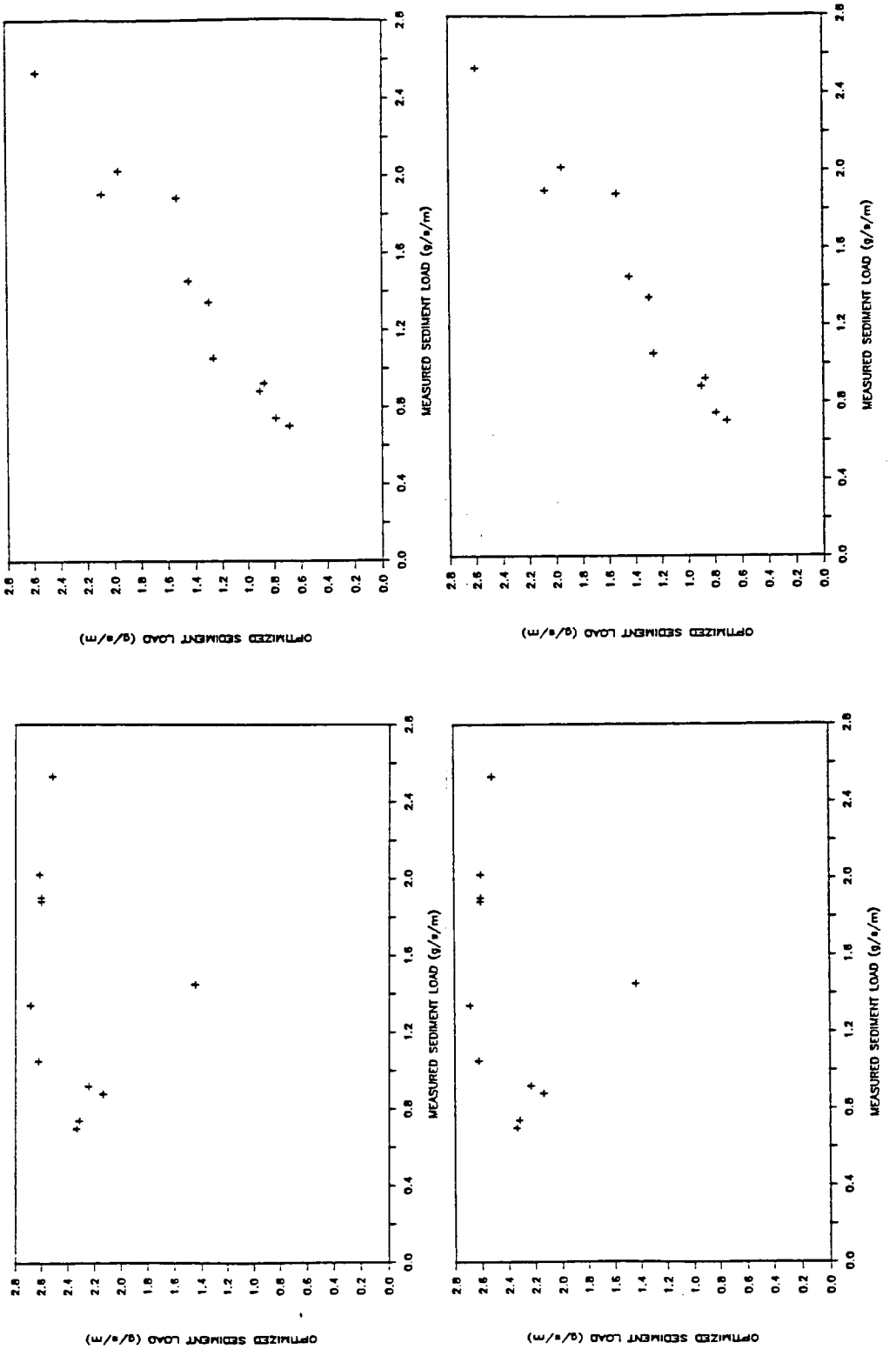

Figure 13. Measured and optimized sediment loads for Grant soil. Optimized values based on a) 2-parameter r_s b) 3-parameter r_s c) 2-parameter r_r and d) 3-parameter r_r calculations.

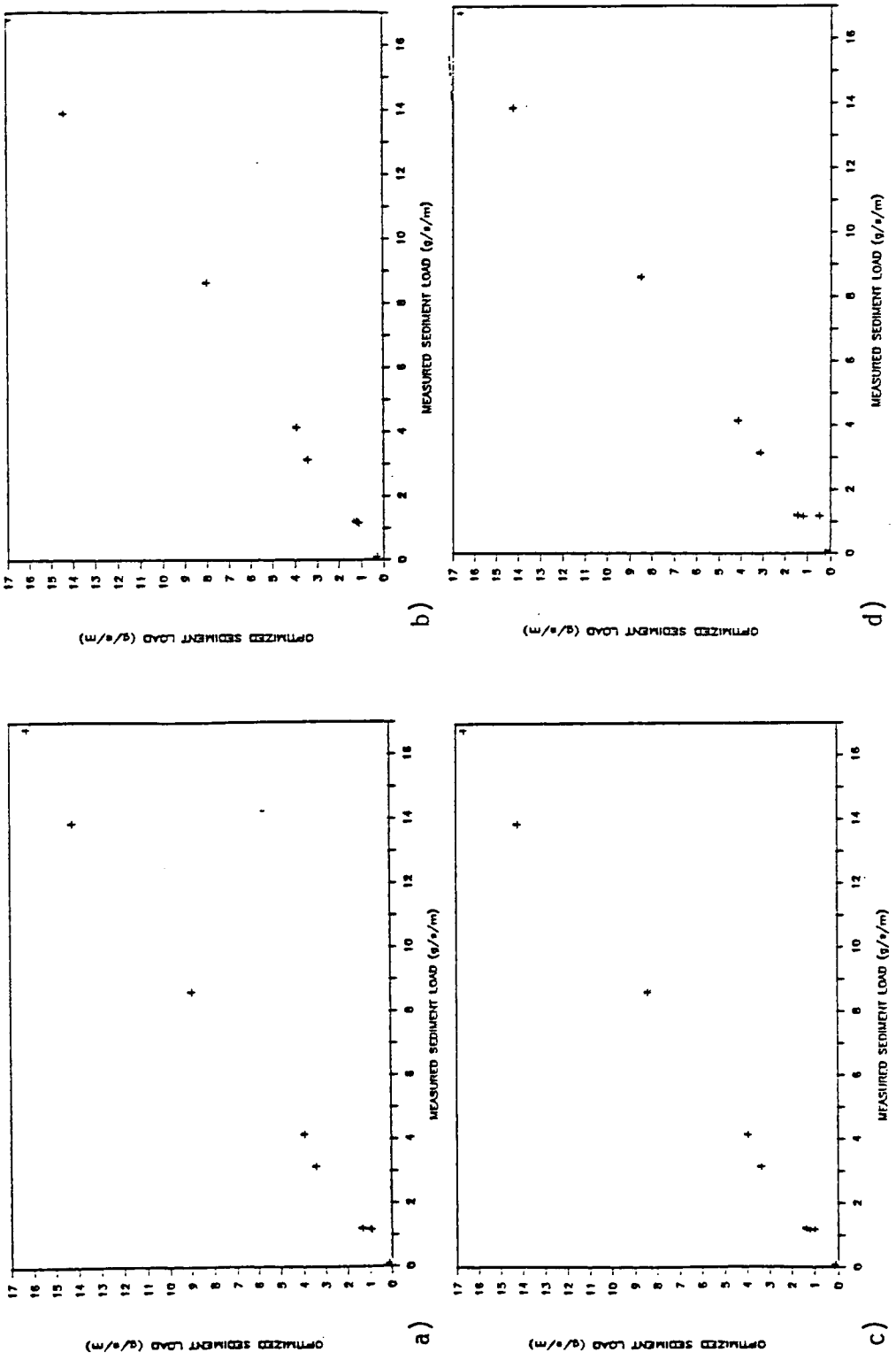

Figure 14. Measured and optimized sediment loads for Pratt soil. Optimized values based on a) 2-parameter r b) 3-parameter r_s c) 2-parameter r_r and d) 3-parameter r_r calculations.

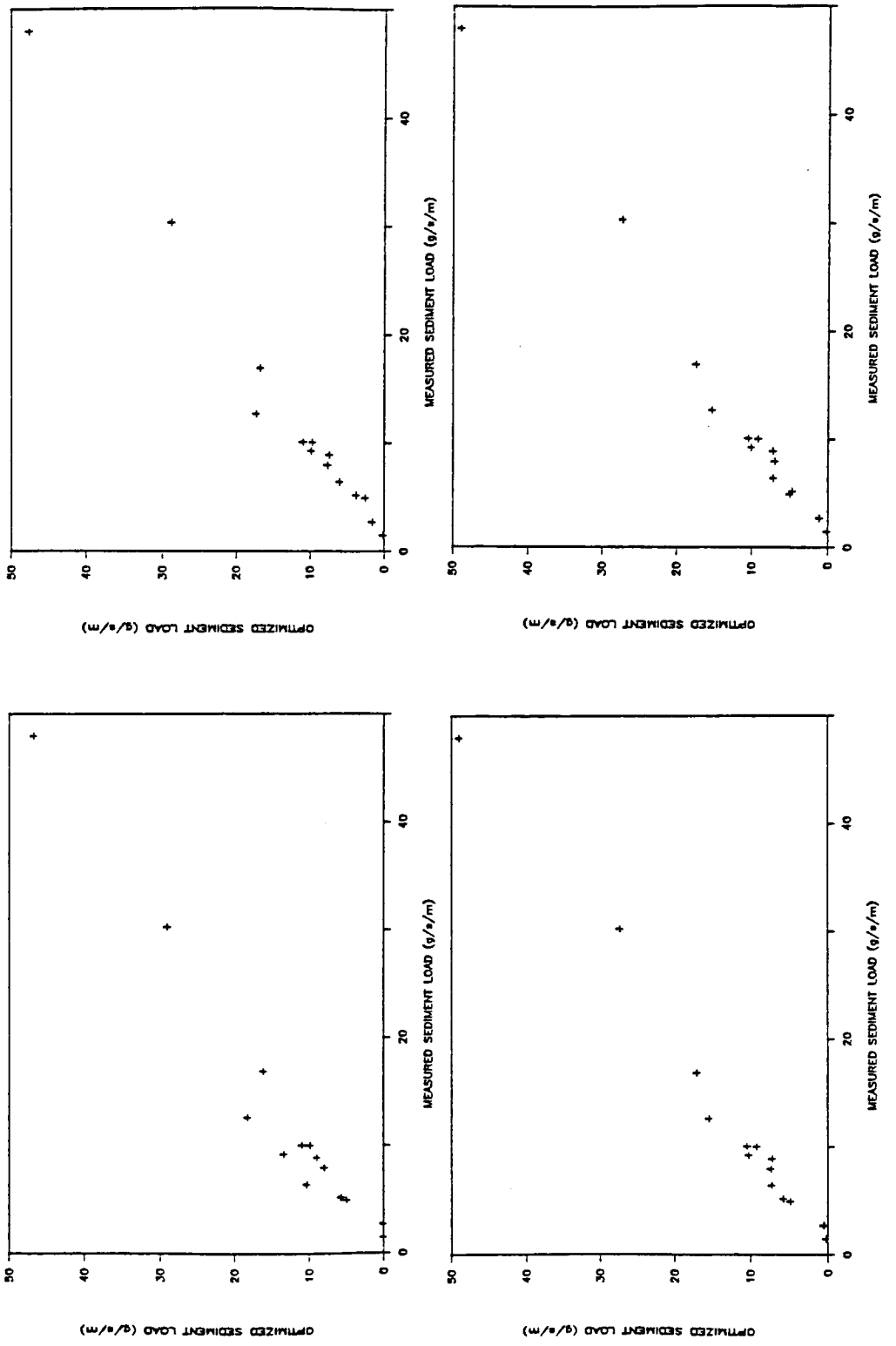

Figure 15. Measured and optimized sediment loads for Degater soil. Optimized values based on a) 2-parameter τ_s b) 3-parameter τ_s c) 2-parameter τ_r and d) 3-parameter τ_r calculations.

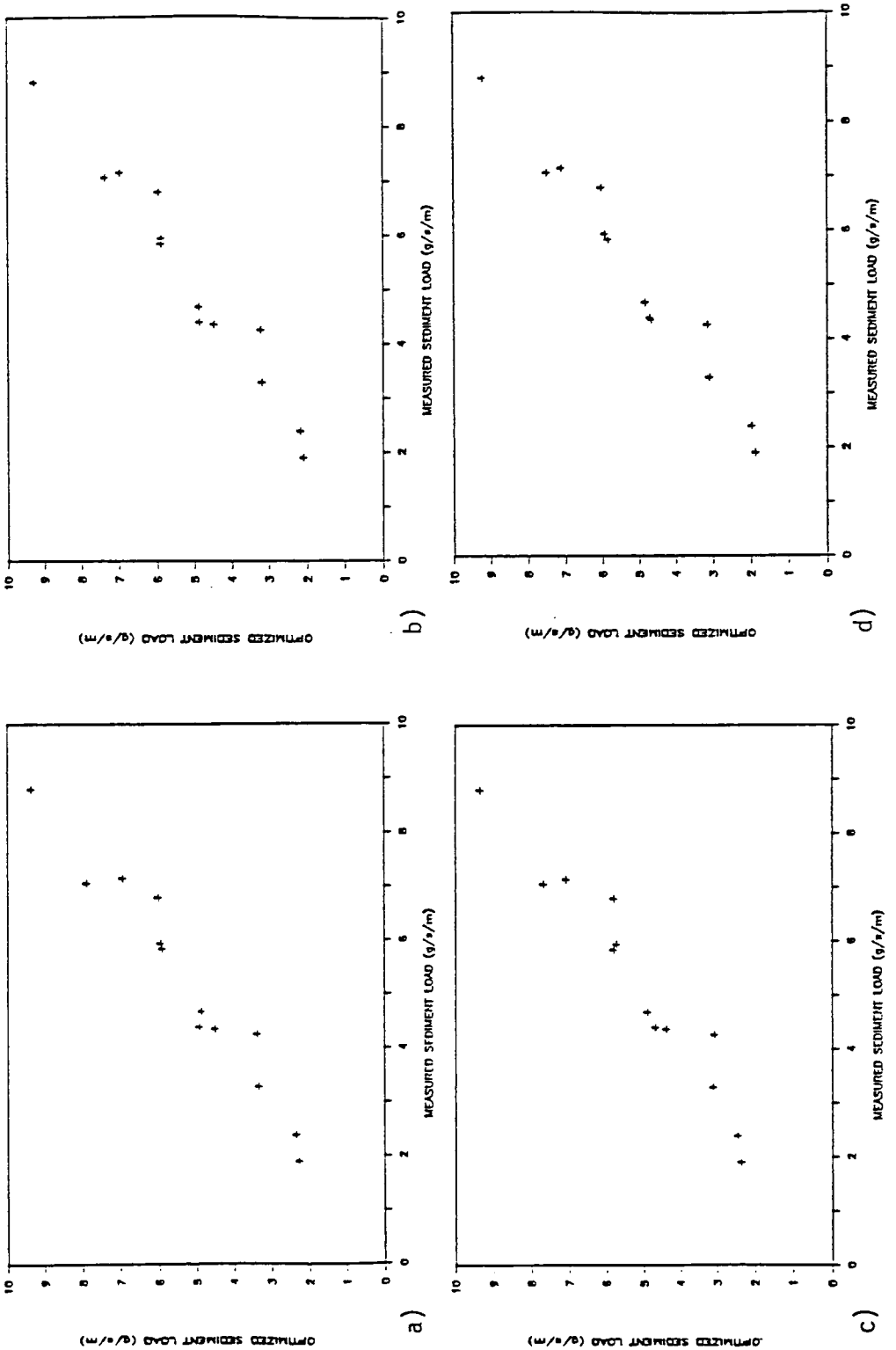

Figure 16. Measured and optimized sediment loads for Pierre soil. Optimized values based on a) 2-parameter r_s b) 3-parameter r_s c) 2-parameter r_r and d) 3-parameter r_r calculations.

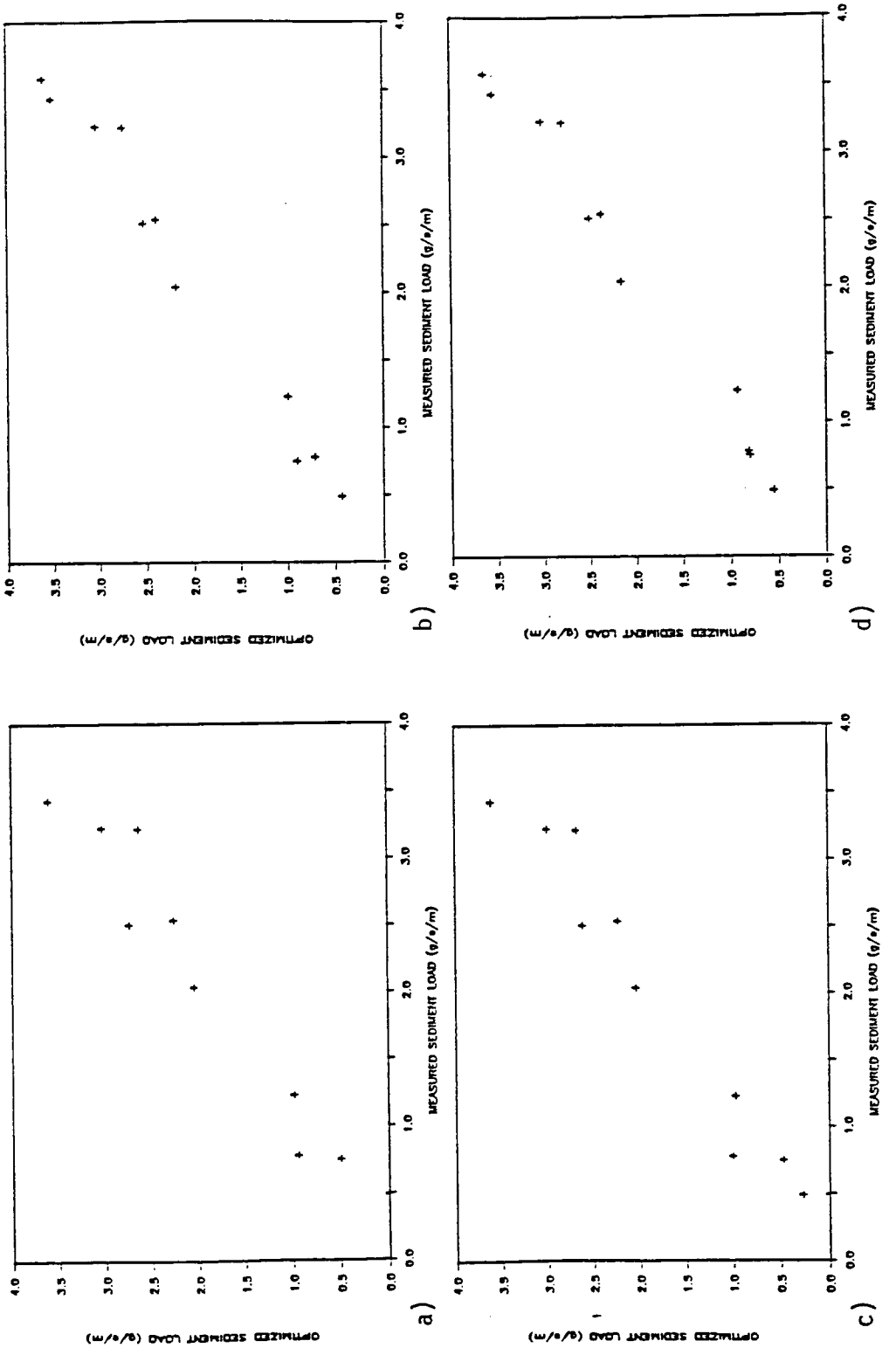

Figure 17. Measured and optimized sediment loads for Querencia soil. Optimized values based on a) 2-parameter τ_r b) 3-parameter τ_s c) 2-parameter τ_r and d) 3-parameter τ_r calculations.

soil runs. The LS values were generally very low, in part because of the low sediment loads (Tables 8-9). The LS for the Degater soil was higher because of high sediment loads. The r^2s for the optimized versus measured sediment loads were about the same for the τ_r and τ_s assumptions (Table 10) for both the 2 and 3-parameter optimizations.

In general, the 3-parameter optimization showed an improvement over the 2-parameter for predicting sediment loads (Table 10). Results were significantly better for the Grant soil plots where the r^2 values went from around .08 to .94 for both the τ_r and τ_s cases and LS values decreased. In this case, the field K_i value used in the 2-parameter optimization was fairly high and the sediment load values were low. The optimization could not find a low enough value for K_r that would result a lower LS value for the data.

These results show that it may be important to use the 3-parameter optimization for the rangeland data. Estimates of the percentage of the total erosion that comes from interrill areas on rangeland plots averaged about 30% for the highest inflow levels compared to 8% for the cropland rills. This much greater contribution by the interrill areas to the sediment load on rangeland plots demonstrates that the K_i value used is relatively more important. The K_i estimated from the interrill plots may not be applicable to the large erosion plots possibly because the cover that is left on the large plots (Table 2) decreases interrill detachment. Although cover was not measured on the interrill plots, their small size made it much easier to remove most of the cover on them than on the large erosion plots.

Table 8. Rangeland parameter and least square (LS) values for rill flow (R) and sheet flow (S) shear stress estimations for the 2-parameter optimization.

SOIL	PLOT	K_i R	K_i S	K_r R	K_r S	τ_c R	τ_c S	LS R	LS S
		$*10^{-6}$	$*10^{-6}$	$*10^{3}$	$*10^{3}$				
		$kg\text{-}s/m^4$	$kg\text{-}s/m^4$	s/m	s/m	N/m^2	N/m^2		
Grant	72	1.039	1.039	0.02	0.00	2.975	0.720	5.61	5.63
	74	1.039	1.039	0.02	0.00	2.988	0.700	8.43	8.46
Pratt	85	0.056	0.056	5.71	1.48	4.741	0.765	0.19	0.61
	89	0.056	0.056	1.68	0.43	4.198	0.642	0.16	0.18
Degater	108	1.553	1.553	8.49	2.45	4.000	0.708	22.13	51.75
	110	1.553	1.553	2.12	0.60	4.630	0.971	7.24	26.20
Pierre	114	0.988	0.988	0.77	0.28	0.556	0.049	1.90	1.78
	116	0.988	0.988	1.47	0.51	3.272	0.778	1.59	1.10
Querencia	131	0.409	0.409	1.00	0.32	3.247	0.741	0.19	0.38
	134	0.409	0.409	0.64	0.18	2.753	0.506	1.83	2.04

Table 9. Rangeland parameter and least square (LS) values for rill flow (R) and sheet flow (S) shear stress estimations for the 3-parameter optimization.

SOIL	PLOT	K_i R $*10^{-6}$ kg-s/m^4	K_i S $*10^{-6}$ kg-s/m^4	K_r R $*10^{3}$ s/m	K_r S $*10^{3}$ s/m	τ_c R N/m^2	τ_c S N/m^2	LS R	LS S
Grant	72	0.477	0.498	0.55	0.17	2.160	0.543	0.20	0.21
	74	0.305	0.296	0.12	0.04	1.687	0.383	0.01	0.00
Pratt	85	0.025	0.136	5.59	1.83	4.650	0.951	0.17	0.71
	89	0.165	0.004	3.66	0.40	5.905	0.556	0.58	0.14
Degater	108	1.654	0.531	8.59	2.63	4.074	0.679	22.07	34.20
	110	1.206	0.675	2.14	0.67	4.136	0.617	5.67	4.66
Pierre	114	0.934	0.889	0.75	0.30	0.222	0.049	1.56	1.46
	116	0.374	0.909	1.04	0.50	0.926	0.741	1.05	1.04
Querencia	131	0.222	0.210	0.78	0.27	2.119	0.469	0.08	0.08
	134	0.272	0.255	0.52	0.17	1.379	0.210	0.74	0.70

Table 10. Rangeland regression analysis results (r^2 values) of optimized vs. measured sediment loads.

SOIL	2 PARAMETER		3 PARAMETER	
	RILL	SHEET	RILL	SHEET
Grant	0.083	0.086	0.946	0.943
Pratt	0.999	0.998	0.998	0.997
Degater	0.986	0.963	0.987	0.982
Pierre	0.935	0.947	0.956	0.954
Querencia	0.899	0.896	0.941	0.944

Comparison of Parameter Values Based on τ_r and τ_s

Croplands

There is no apparent relationship between K_i estimated from τ_r and from τ_s as shown in Fig. 18 and Table 11 (r^2=0.0007). K_i estimated from τ_r optimized to the smallest value allowed by the optimization (4115 kg-s/m^4) for several rills in different soils. The large coefficient of variation (CV) for the τ_r K_i of Amarillo soil (Table 6) is due to these low K_i values.

Figure 19 shows that K_r values estimated from τ_s were much lower than K_r values estimated from τ_r for both the 2- and 3-parameter optimizations. The K_r values estimated from τ_r were about 3 times larger than those estimated from τ_s for the 2-parameter optimization and about 2.5 times larger for the 3-parameter. The data show linear relationships of K_r values estimated from τ_r and τ_s with r^2 values of 0.85 and 0.78 for 2- and 3-parameter optimizations respectively (Table 11).

Figure 20 shows no apparent relationship between τ_r and τ_s estimated values of τ_c for either the 2 or 3-parameter optimizations. In general τ_s τ_c values were lower than τ_r τ_c values except when τ_c was optimized to zero (or a very low value). The τ_c value was not allowed by the optimization to go below zero because a negative τ_c would not make physical sense nor would the model accept a negative τ_c value. This restriction on τ_c may help explain the relatively large difference between τ_r and τ_s LS values for Heiden rills 1 and 5 and Walla Walla rill 4 (Tables 3 and 5). A large difference in the τ_r and τ_s CVs was found for several soils (Table 4: Amarillo and Heiden; Table 6: Sharpsburg and Heiden). This occurred when the τ_r τ_c of one or more of

Table 11. Regression analysis results (r^2 values) for various combinations of the optimized parameter values.

PARAMETER	TYPE	ANALYSIS	RANGELAND	CROPLAND
K_i	3 Parameter	Rill vs. Sheet	0.313	0.0007
K_r	2 Parameter	Rill vs. Sheet	0.993	0.853
K_r	3 Parameter	Rill vs. Sheet	0.915	0.710
τ_c	2 Parameter	Rill vs. Sheet	0.757	0.424
τ_c	3 Parameter	Rill vs. Sheet	0.376	0.480
K_r	Rill	2 vs. 3 Parameter	0.941	0.938
K_r	Sheet	2 vs. 3 Parameter	0.986	0.973
τ_c	Rill	2 vs. 3 Parameter	0.685	0.832
τ_c	Sheet	2 vs. 3 Parameter	0.584	0.298

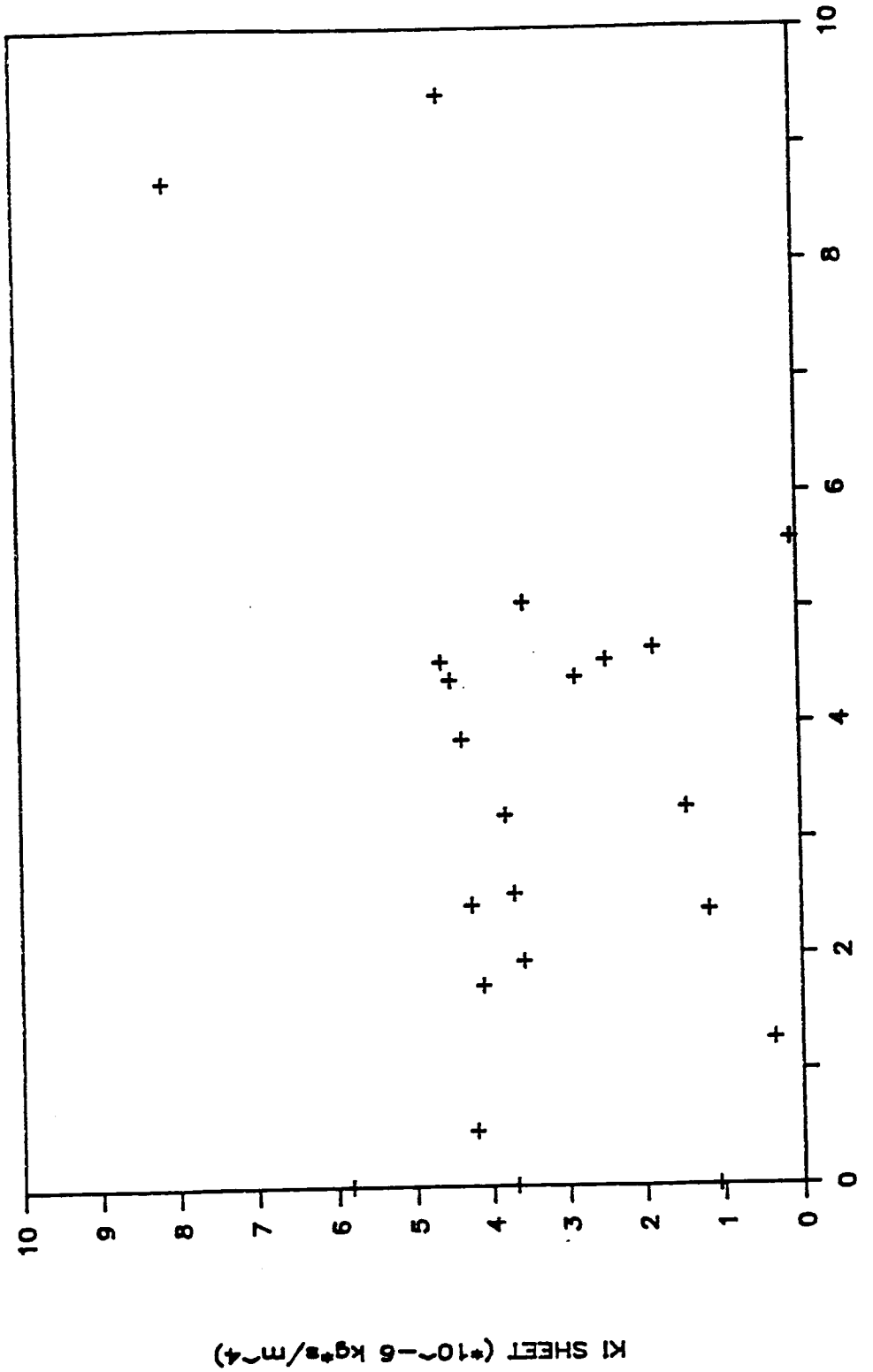

Figure 18. Cropland r_r K_i and r_s K_i values for the 3-parameter optimization.

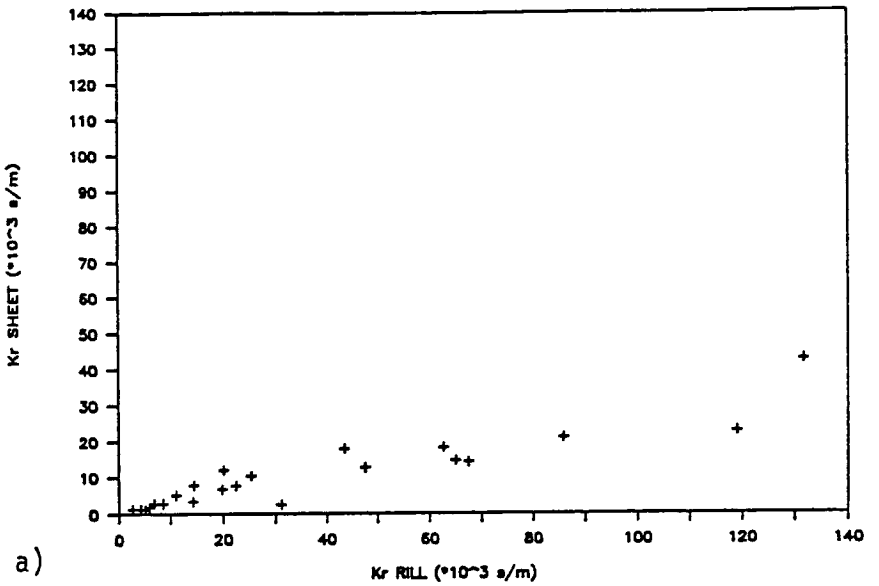

a)

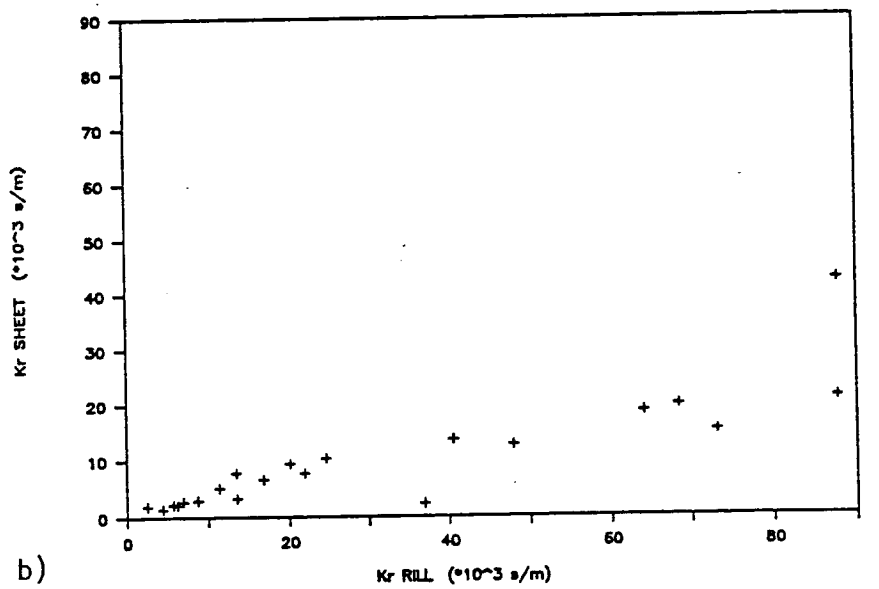

b)

Figure 19. Cropland $\tau_r K_r$ and $\tau_s K_r$ values for the a) 2-parameter and b) 3-parameter optimizations.

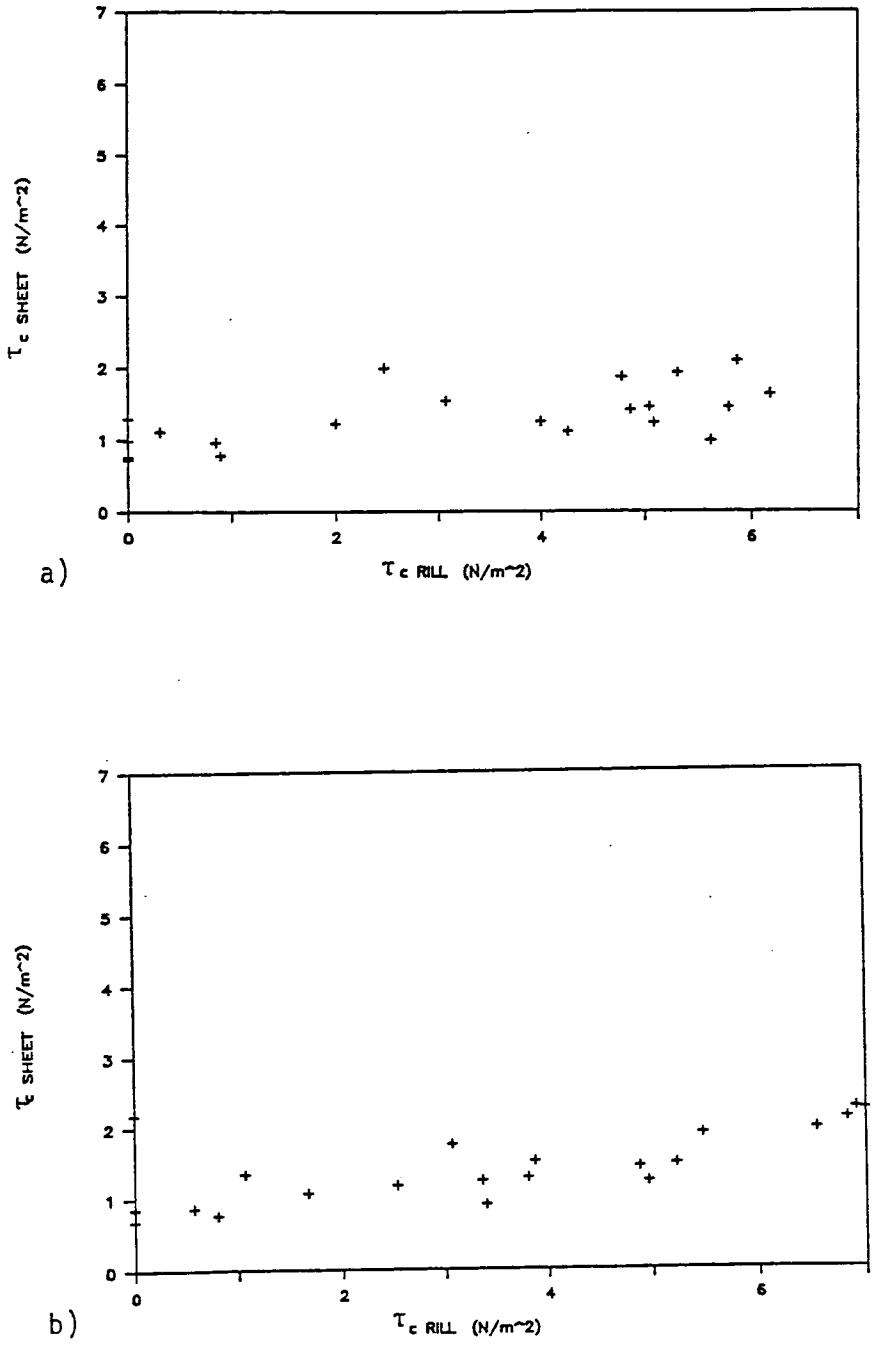

Figure 20. Cropland τ_r τ_c and τ_s τ_c values for the a) 2-parameter and b) 3-parameter optimizations.

the rills for that soil optimized to 0 while the others did not.

Rangelands

The K_i values for τ_r and τ_s from the 3-parameter optimization show no apparent trend (r^2=.313 Table 11 and Fig 21). Values of K_i estimated from τ_s and τ_r were similar for both plots on Grant and Querencia soils and for Pierre soil plot 114. K_i values for the Pratt plots, though not the same for τ_r and τ_s, were lower than the other sites. Degater τ_r values of K_i were the highest of the rangeland soils tested but the τ_s values of K_i were about 1/2 to 1/3 of the τ_r K_i values.

Figure 22 shows K_r from τ_s much lower than K_r from τ_r for both the 2- and 3-parameter optimizations. Regression analysis shows a strong linear relationship between K_r values from τ_r and from τ_s with r^2=0.993 and 0.915 for 2- and 3-parameter optimizations respectively (Table 11). The K_r values for τ_r were about 3.6 (2-parameter) and 3.1 (3-parameter) times higher than the corresponding values for τ_s.

The τ_c values for τ_r and τ_s for the 2-parameter optimization are presented in Figure 23a. They show a linear relationship between τ_c values for τ_r and τ_s (r^2=0.757, Table 11). The τ_r τ_c values were generally about 4 times the τ_s τ_c values. For the 3-parameter optimization (Fig. 23b) there was no apparent relationship between τ_r and τ_s τ_c values (r^2=.376 Table 11) although τ_s τ_c values were much lower than τ_r τ_c values.

Comparison of 2 and 3-parameter Optimization Parameter Values

Croplands

Optimized K_i values vary widely for different rills within one soil (Table 5). They do not appear to be related to the calculated K_i for a

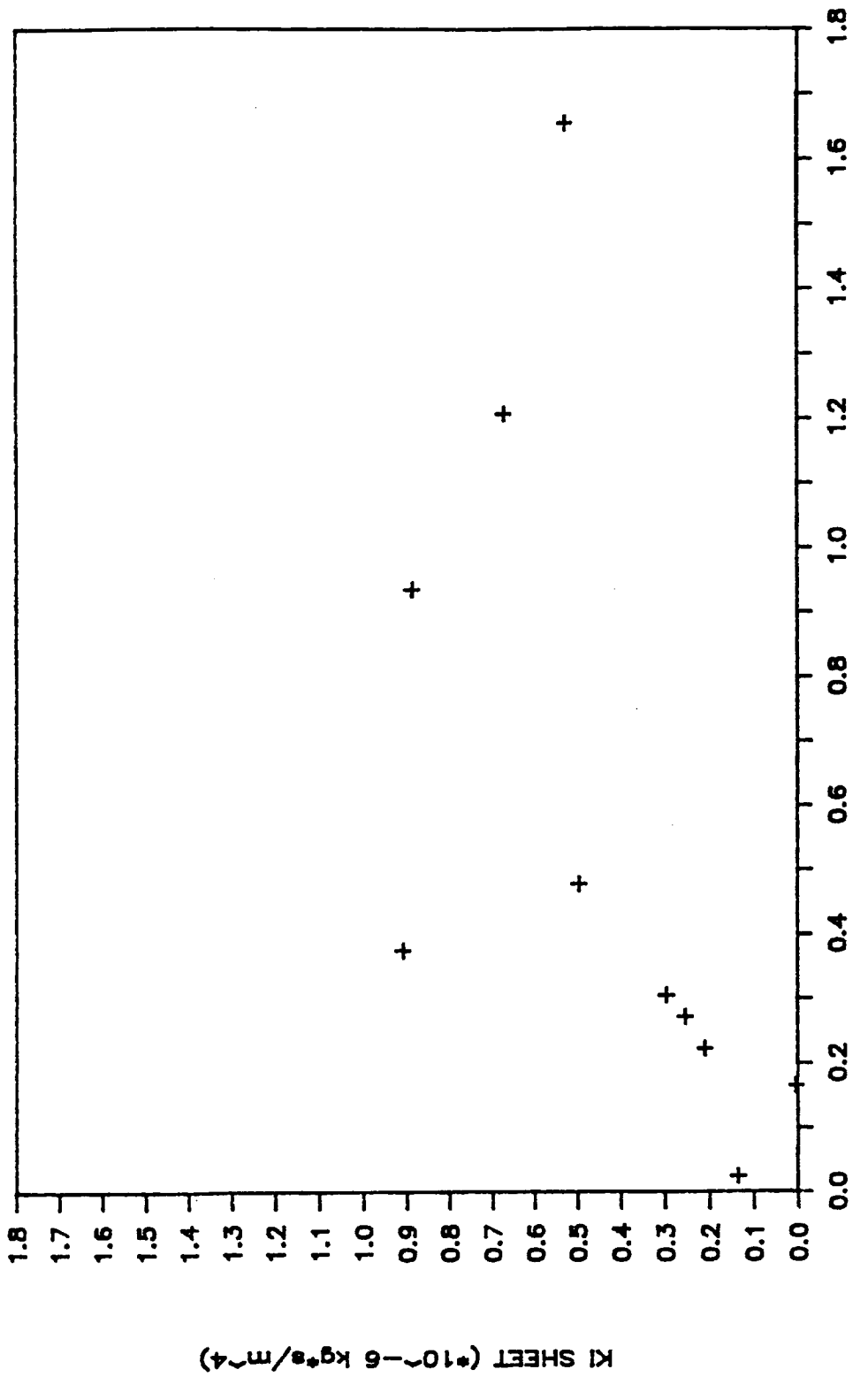

Figure 21. Rangeland r_r K_i and r_s K_i values for the 3-parameter optimization.

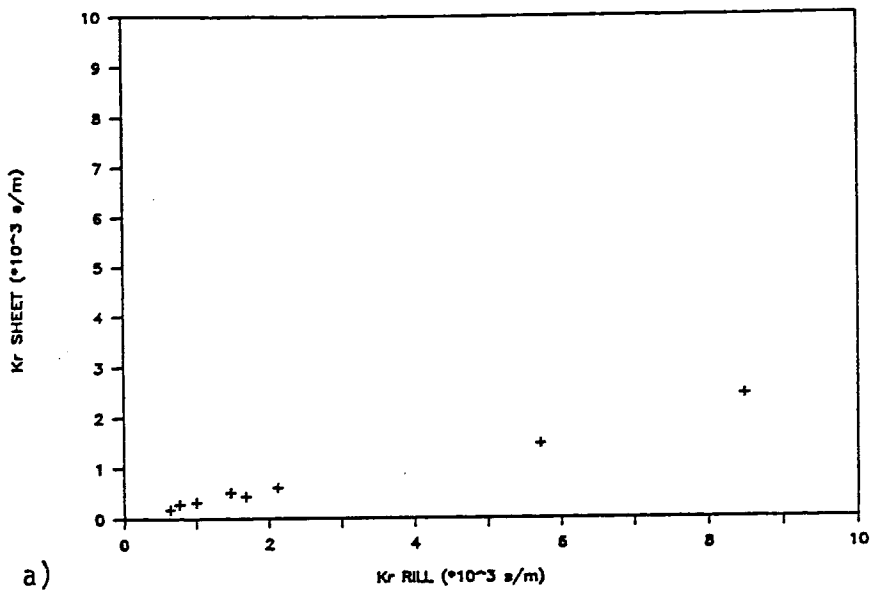

a)

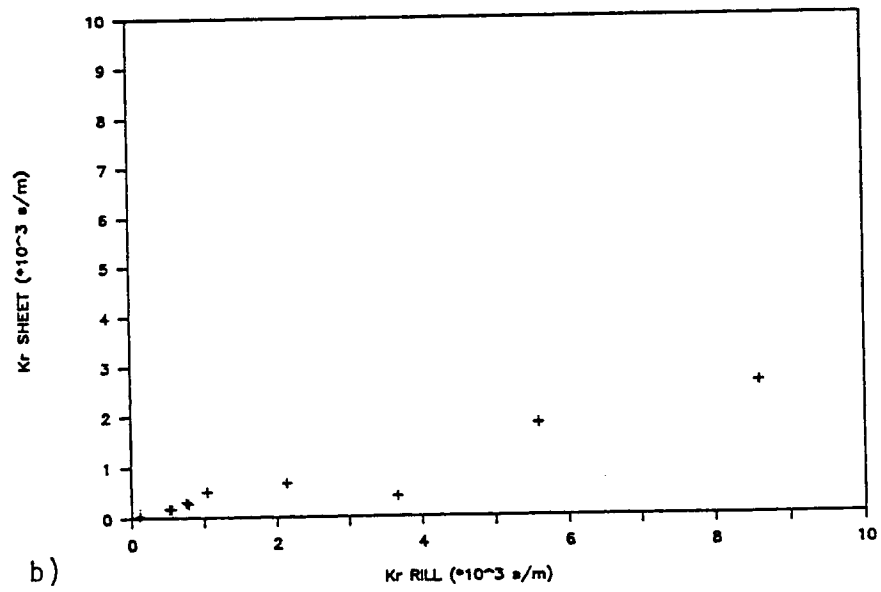

b)

Figure 22. Rangeland τ_r K_r and τ_s K_r values for the a) 2-parameter and b) 3-parameter optimizations.

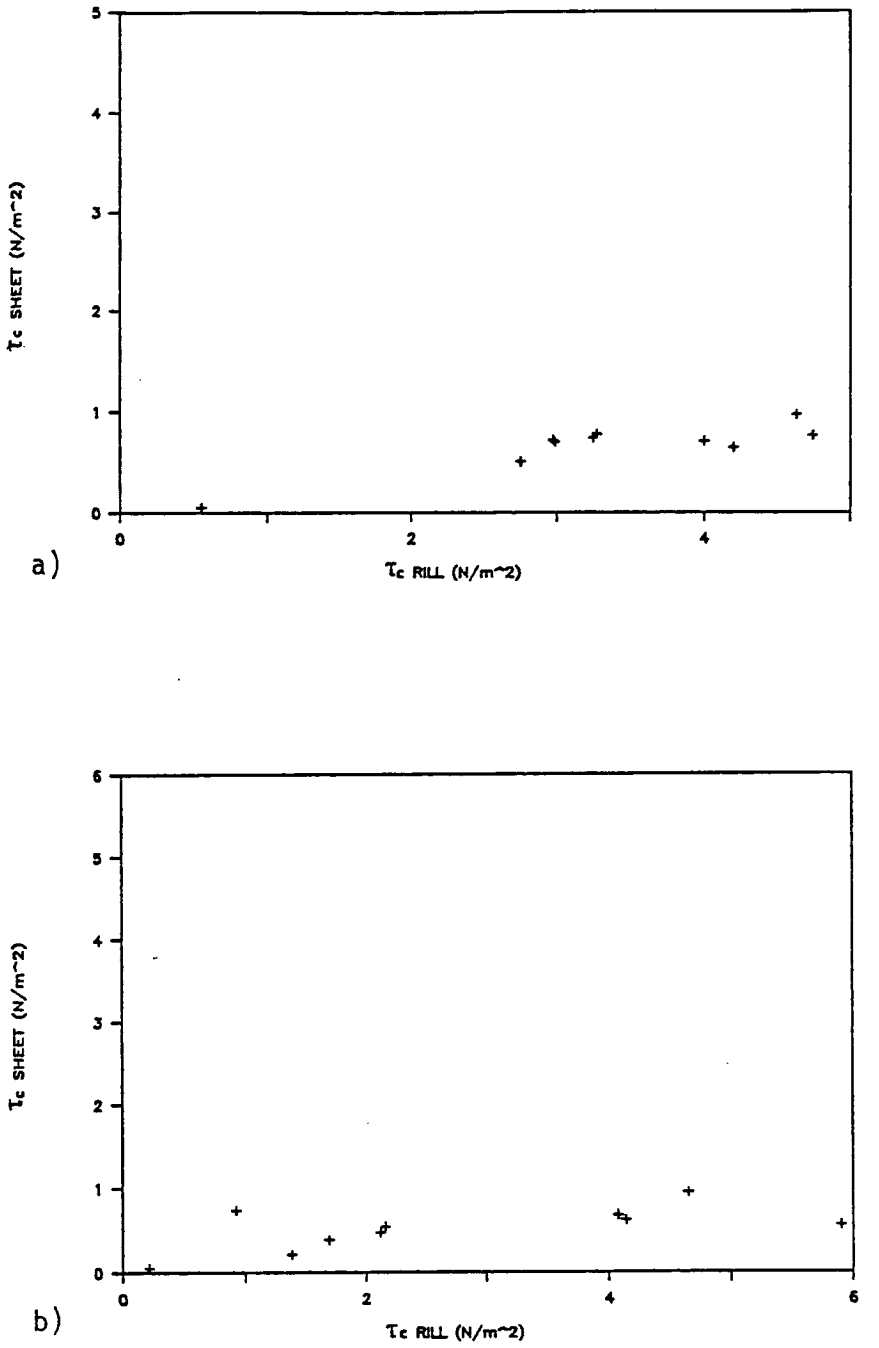

Figure 23. Rangeland τ_r τ_c and τ_s τ_c values for the a) 2-parameter and b) 3-parameter optimizations.

site. Since the 2 and 3-parameter optimizations predicted about the same sediment loads, this could indicate that the optimization is insensitive to K_i. It also reflects the relatively small contribution interrill detachment makes to the sediment load in these particular experiments.

Figure 24 shows that the K_r values obtained from the 2-parameter optimization are about the same as those from the 3-parameter. One exception was the 2-parameter K_r value for Walla Walla rill 5 which was about 1.6 times larger that the corresponding 3-parameter τ_r K_r value. The r^2 values of the 2- and 3-parameter K_r values were 0.938 and 0.973 for τ_r and τ_s respectively (Table 11) indicating relatively good agreement between the optimizations.

There was no apparent relationship between 2 and 3-parameter τ_s τ_c values (Fig. 25a) (r^2=.297 Table 11). The τ_r τ_c values (Fig. 25b) show a fairly good linear relationship between 2 and 3-parameter optimizations (r^2=.802, Table 11). The τ_r τ_c values were about the same for the 2 and 3-parameter optimizations even when τ_c was optimized to zero.

Rangelands

Tables 7 and 8 show that in most cases, both τ_r and τ_s K_i optimized values were lower than K_i values estimated from field data on the small plots. As discussed earlier, this is possibly because of the greater amount of ground cover left on the large plots. The field estimated and optimized K_i values for τ_r follow a similar trend with the highest K_i values for the Degater soil and the lowest for the Pratt. There was no similar trend for the τ_s K_i values. Optimization of the τ_s K_i for the

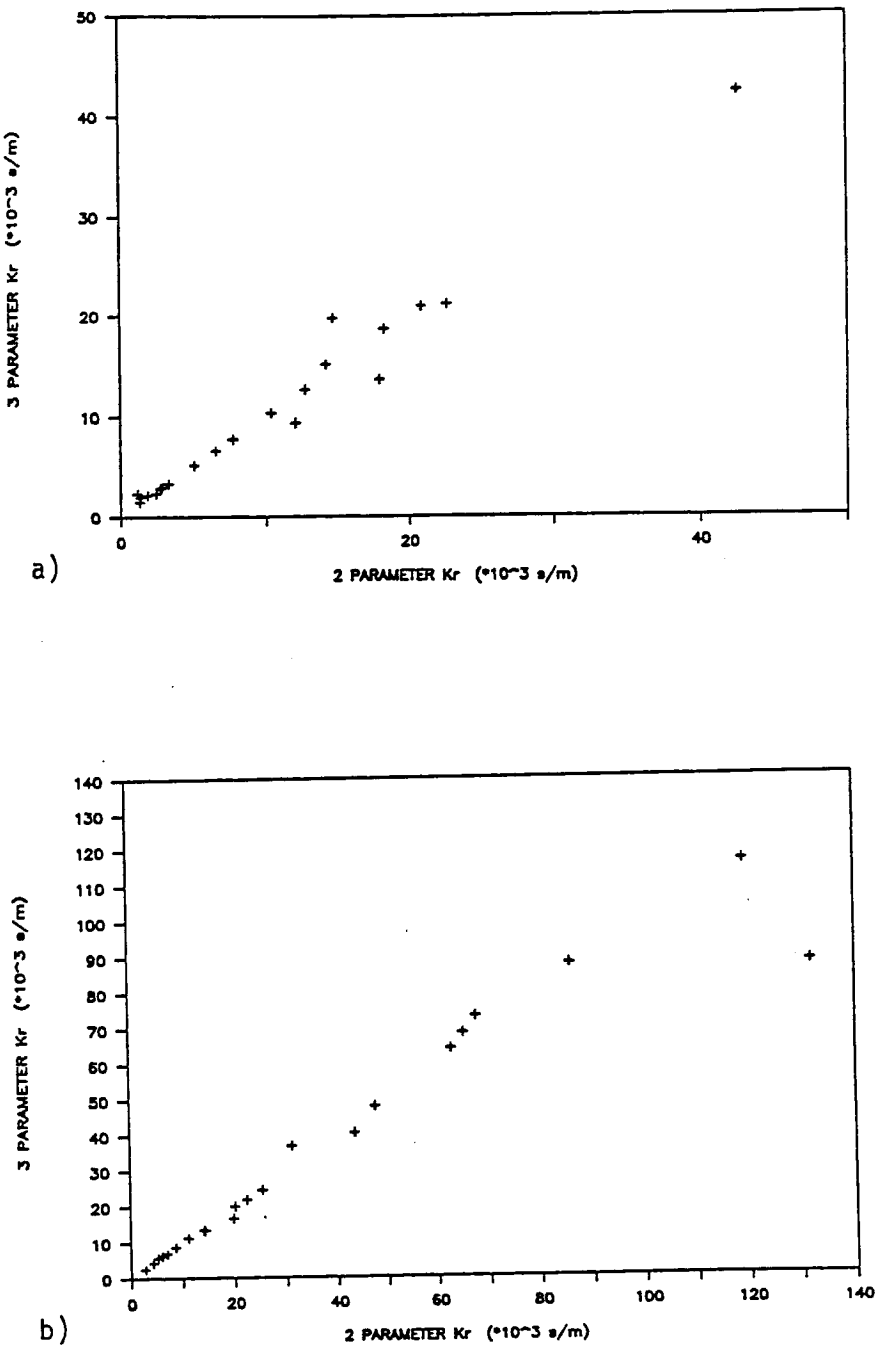

Figure 24. Cropland K_r values obtained from 2- and 3-parameter optimizations for a) τ_s and b) τ_r.

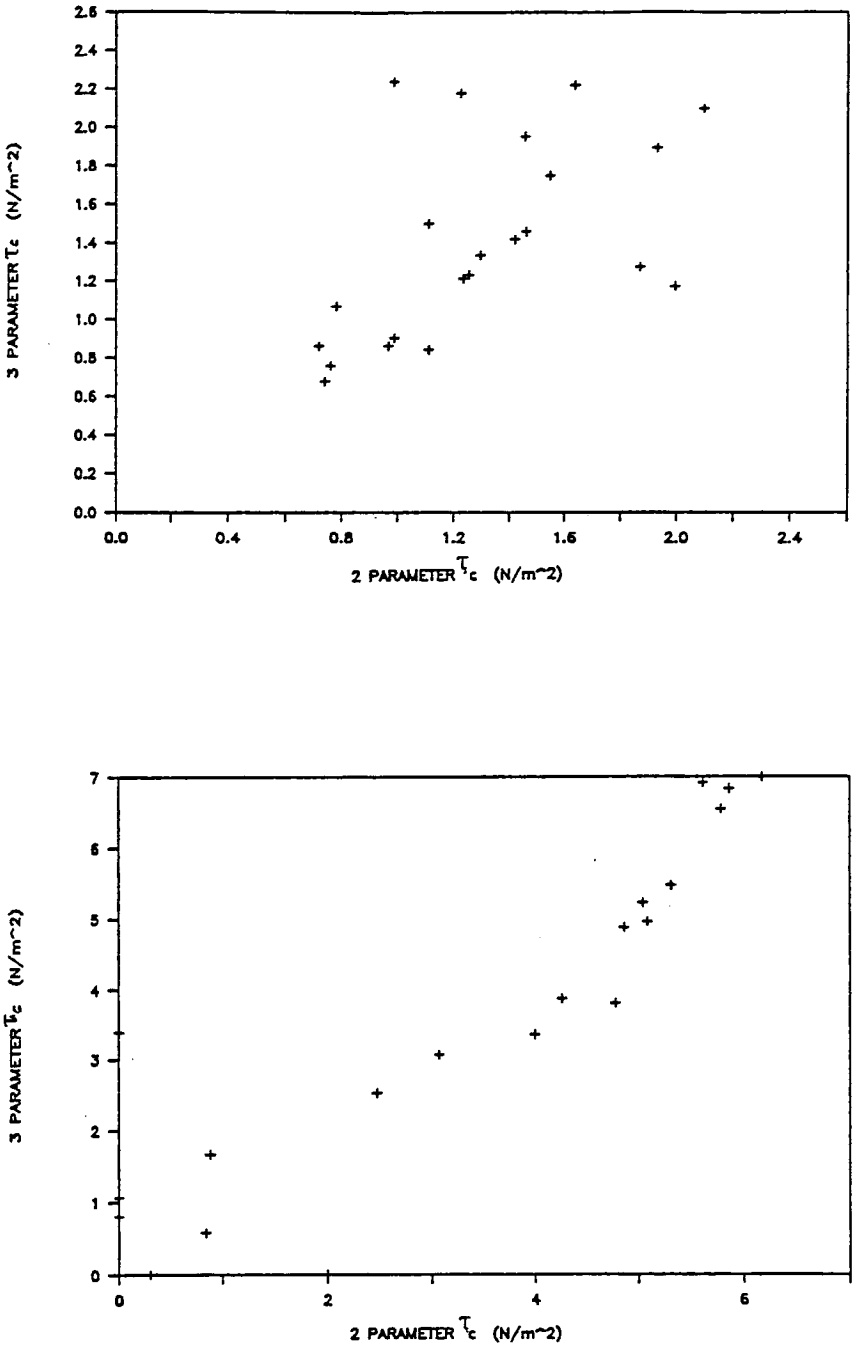

Figure 25. Cropland τ_c values obtained from 2- and 3-parameter optimizations for a) τ_s and b) τ_r.

Degater plots and the τ_r and τ_s K_i values for the Grant plots led to lower values than the field estimated K_i and improved the LS values.

The K_r values from the 2 and 3-parameter optimizations are shown to be very close (Fig. 26) for both τ_r and τ_s K_rs. Linear regression of the 2 and 3-parameter K_r values confirm this relationship with r^2 values of 0.941 for τ_r K_r and 0.986 for τ_s K_r (Table 11).

Figure 27 shows no strong linear relationship between 2 and 3-parameter τ_c values for either τ_r or τ_s assumptions (r^2=0.685 and 0.584 respectively, Table 11). In general, the 2- and 3-parameter τ_c values were similar or the 2-parameter values were slightly higher for both the τ_r and τ_s cases.

Discussion of Parameter Values

The cropland and rangeland results show that the rill detachment parameter (K_r and τ_c) values for the τ_s model were much lower than the τ_r model. Overall, K_r values were generally 2.5 to 3.5 times lower for the τ_s model than the τ_r model. The τ_c values estimated from τ_s were 2.25 to 5.25 times lower than τ_r τ_c values. These lower parameter values are the result of the shear stress being underestimated when calculated from sheet flow. A low value of τ would force the τ_c to be lower in order to get the same amount of sediment detachment. The decrease in τ_c then forces a decrease in K_r to maintain the same erosion rate over the area.

The optimized K_i values for croplands covered about the same range and were not consistantly larger for the τ_r or the τ_s models. For the rangeland soils, K_i values were generally lower for the τ_s case. This reflects the relatively greater contribution of interrill erosion in the

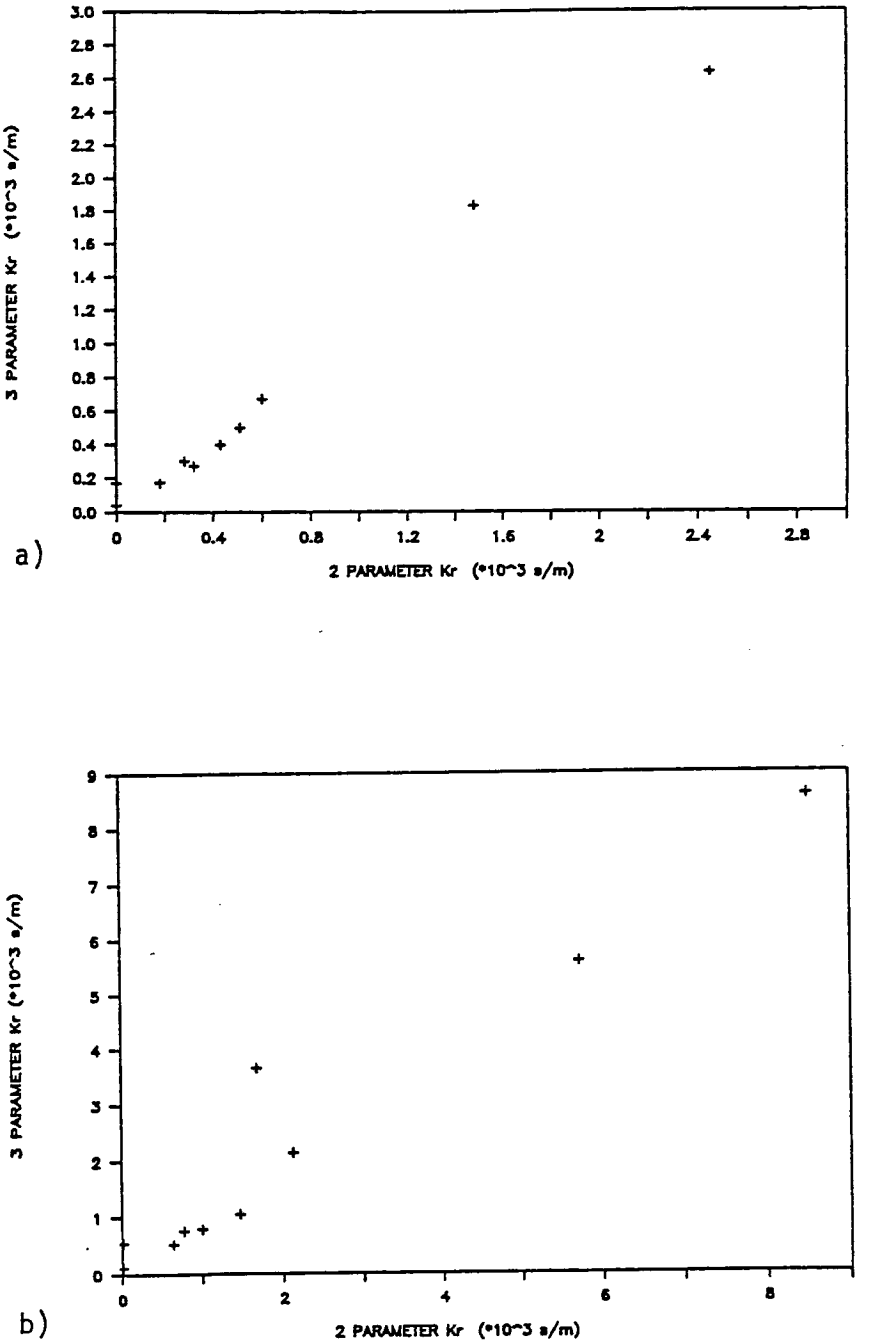

Figure 26. Rangeland K_r values obtained from 2- and 3-parameter optimizations for a) τ_s and b) τ_r.

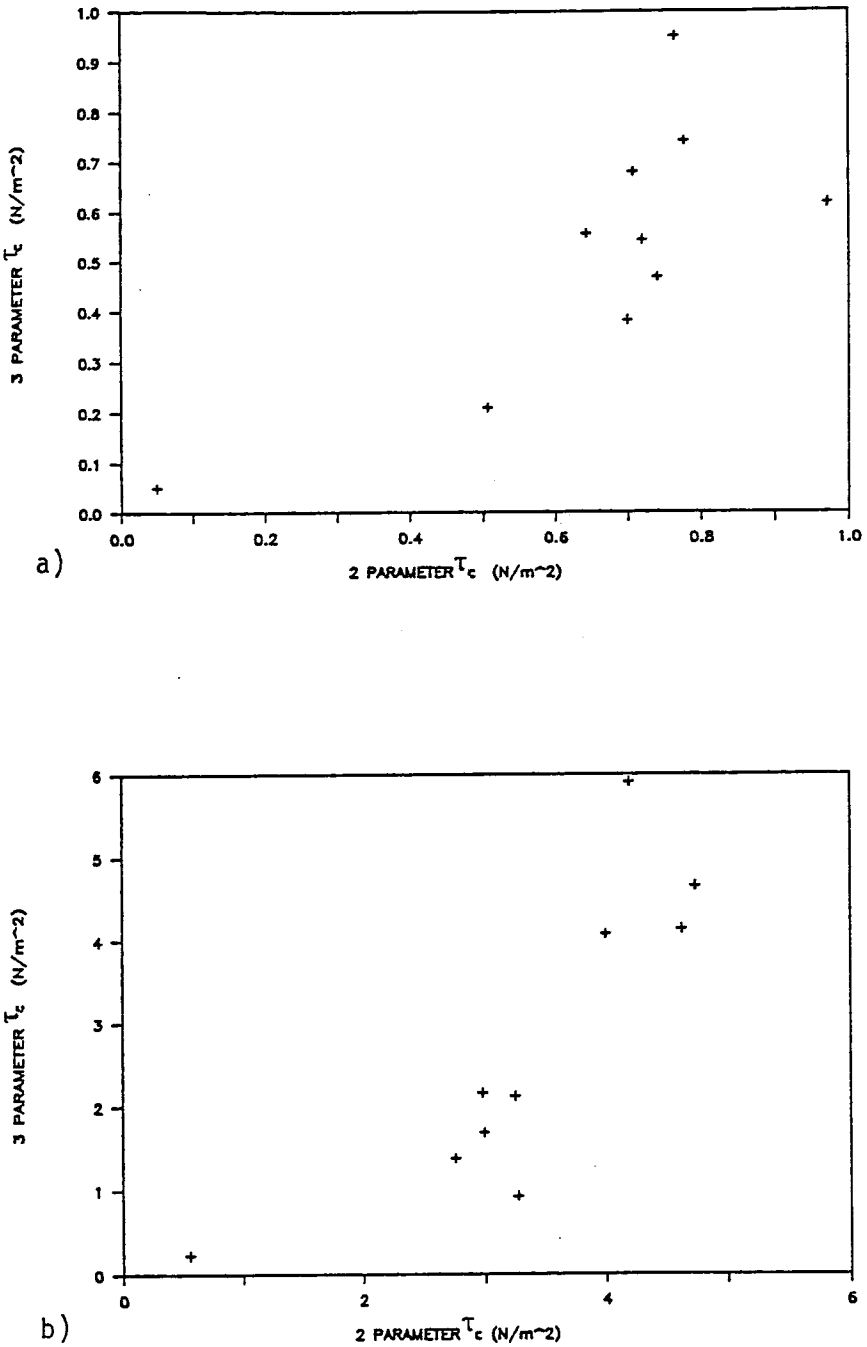

Figure 27. Rangeland τ_c values obtained from 2- and 3-parameter optimizations for a) τ_s and b) τ_r.

rangeland experiments.

It was previously determined that the use of the sheet flow assumption would underestimate the actual shear stress in a rill. These results show that the optimal values of K_r and τ_c for the sheet flow assumption are distorted by factors of 3 and 5, respectively, from the corresponding K_r and τ_c values for partitioned sheet and rill flow. Although the optimization with the uniform sheet flow model can fit the observed data well, the K_r and τ_c parameters are distorted and there is no apparent mechanism to adjust them as rill density or rill properties change.

The inability of the distorted parameter values to account for changing conditions was tested on an example data set (Sharpsburg rill 1). Using the optimized K_r and τ_c values for partitioned flow, the WEPP model was run with a rill spacing of 4.0 m. The predicted sediment loads, which were 12-50% higher than the original rill spacing (.48 m), were then used as the measured values for optimization of both the τ_r and τ_s models to see if the optimal parameter values changed. For partitioned flow, optimized K_r and τ_c values were the same for both rill spacings. For the sheet flow case, the optimal K_r was about the same for both rill spacings but the optimal τ_c value decreased by about 1/3 (1.46 to 0.934 N/m^2).

When sheet flow is assumed there is no mechanism to account for the change in the amount of flow in a rill as rill spacing increases. To obtain the higher sediment loads found when rill spacing increases, one or both of the parameters must decrease to get more detachment. This is important because, if shear stress is estimated from sheet flow, parameter values must be readjusted every time rill spacing or other

rill characteristics are changed. When the flow is partitioned and the rill spacing increases, the flow into the rills will increase so the parameter values will not have to be readjusted every time rill characteristics change.

The K_i and K_r parameter values for croplands were generally higher than rangelands. This was expected since the cropland sediment loads were higher because the soil had been tilled before the experiments allowing for more detachment. Although τ_c values might be expected to be lower for croplands, they covered about the same range for cropland (0-7 N/m^2) and rangeland (0-6 N/m^2) soils.

CHAPTER 5

CONCLUSIONS, RECOMMENDATIONS, FURTHER WORK

Summary and Conclusions

The first part of this study showed that the shear stress in a rill would be greatly underestimated if the flow is assumed to be uniform sheet flow. This is important in erosion modeling for two reasons. The first is that detachment is assumed to only occur if the shear stress of the flow exceeds the critical shear stress of the soil. If the shear stress is underestimated, detachment will not be expected and sediment loads will be underpredicted. Also, the distance down a hillslope that rills would be expected to start would be overestimated. The second reason is that the transport capacity of the flow depends on the shear stress and, if underestimated, would lead to further errors in estimates of the rill detachment rates.

The second phase of the study showed that the distance between rills and the rill width affect the predicted sediment loads from the WEPP erosion model. As the rill spacing increases, more flow is routed to each rill increasing the shear stress of the flow. If this shear stress exceeds the critical shear stress, detachment by flow can occur and sediment loads increase. Accurate estimation of rill spacing is important in erosion modeling since it could lead to underestimation of sediment loads if the rill spacing is too low and overestimation if it is too high.

The effect of increased rill width on sediment loads is the result of the interaction of increasing the area available for detachment and decreasing the shear stress of the flow. When the shear stress of the flow easily exceeds the critical shear stress, increased rill width

leads to more detachment because of the increased area the flow acts upon. When the flows' shear stress is close to the critical shear stress and rill width increases, the decrease in shear stress will be more important than the added area available for detachment and detachment will decrease. This is a complicated interaction and it demonstrates the importance of accurate estimation of rill width for erosion modeling.

The third part of this study involved the use of optimization techniques to obtain erodibility parameter values for two versions of an erosion model. One version estimated shear stress from thin sheet flow and the other estimated shear stress from flow partitioned into rill and interrill areas. The optimization found parameter values that could closely predict the observed sediment loads for both versions. It was concluded that optimization could be used to find parameter values for both erosion models.

The optimization for the two versions differed in the parameter values obtained. Values for the rill detachment parameters (K_r and τ_c) were generally found to be lower for the model that estimated shear stress from sheet flow. It was concluded that using shear stress estimates based on sheet flow would have a large impact on erosion model parameters. Since it was determined that shear stress estimates based on partitioned flow were more accurate than those based on sheet flow, it was concluded that, for erosion modeling, parameter values should be estimated with a model that uses partitioned flow to calculate shear stress. Another reason to use partitioned flow for parameter estimation, based on this study, is that when flow is partitioned and rill spacing increased, flow into rills will increase so that parameter

values need not be adjusted as rill spacing changes. However, if shear stress is estimated using the sheet flow assumption, parameter values must be readjusted every time rill spacing changes.

Recommendations

Development of appropriate parameter values is important to the successful application of the erosion model. In this case, optimization of field data is the method chosen to find erodibility parameter values for the tested soils. These parameter values can then be related to soil and other physical properties to establish their values for untested soils.

Because of the different conditions found on cropland and rangeland sites the experiments tested for slightly different things. For the cropland experiments, the K_i estimated from the small plots is a better estimate than the one estimated from the rill data. In the rill data, the dominance of the sediment from rill detachment reduces the ability to estimate interrill detachment and thus, K_i. It is recommended that because K_i is more sensitive to the small plot data, the 2-parameter optimization should be used for the croplands experiment data. On the large rangeland plots, interrill erosion contributes a greater percentage of the sediment than on croplands so K_i is more accurately determined with the 3-parameter optimization.

It is also important in optimization to have a good set of starting values for the parameters. This allows the optimization to run faster and helps to assure that a global minimum LS is reached. There were several times when data sets had to be rerun because it was apparent that they had not reached a minimum. If it is suspected that the

optimization did not reach a minimum, the optimized parameter values from the first run may be used as starting values for a second run.

Further Work

After the erodibility parameter values are established for all the test plots, the next step in the model development will be to relate them to soil properties. Possibilities include soil textural data, soil shear strength, soil chemistry and mineralogy.

Rill transport is primarily responsible for movement of water and sediment from an upland area. To accurately estimate the erosion from both interrill and rill areas it is important to be able to estimate how many rills will develop under a certain set of conditions. In the current study, the cropland sites had preformed rills a fixed distance apart (0.48 m) while the distance between rills on rangeland plots could only be estimated since it was not known where or if they would form. More information is needed on estimating rill formation including the number and geometry of the rills that develop on rangeland plots. Geometry data were taken from cropland rills but were not available at the time of the study. When the geometry data become available they can be used to test the validity of the assumptions on rill geometry used in the model.

Also needed is investigation of friction factors for rangelands sites. One value was used for all sites in this study. Plots have both rill and interrill areas; using one friction factor for the entire plot is not adequate for describing both areas. Velocity studies in concentrated flow areas on the rangeland plots were only done for two sites (which resulted in the 1.7 value for total f that was used).

Velocity measurements were obtained at each cropland site by adding dye to the flow in two of the rills.

Other areas for improving rill erosion estimates include understanding more about the individual rill detachment subprocesses (headcutting, undercutting and slumping, and scour by shear stress acting on the rill boundary). Current models lump them all into a detachment equation which describes scour. Describing these subprocesses will also require a better understanding of rill hydraulics and better soil mechanical descriptions of sidewall sloughing.

APPENDIX A

Table 1. Data inputs to model for Sharpsburg soil.

RILL	INTENSITY	INFLOW	Q	VELOCITY	MEASURED SEDIMENT LOAD
	mm/hr	l/min	l/min/m	m/s	g/s/m
1	58.39	0	8.13		
	58.39	8	19.47	0.21	9.81
	58.39	16	32.36	0.26	11.58
	58.39	24	32.04	0.26	12.92
	58.39	32	56.09	0.28	32.15
	58.39	40	68.55	0.30	32.06
2	58.39	0	5.58		
	58.39	8	18.68	0.19	10.54
	58.39	16	31.69	0.25	17.63
	58.39	24	32.32	0.25	14.42
	58.39	32	57.09	0.26	32.83
	58.39	40	68.77	0.30	39.81
3	58.39	0	3.75		
	58.39	8	15.65	0.17	7.44
	58.39	16	38.62	0.24	17.83
	58.39	24	41.34	0.25	27.63
	58.39	32	66.05	0.29	56.31
	58.39	40	84.39	0.28	67.40
4	58.39	0	3.73		
	58.39	8	8.11	0.14	5.29
	58.39	16	29.76	0.22	18.19
	58.39	24	30.68	0.21	17.19
	58.39	32	53.24	0.26	58.00
	58.39	40	73.75	0.28	59.92
5	58.39	0	5.98		
	58.39	8	16.97	0.23	11.71
	58.39	16	31.12	0.26	15.35
	58.39	24	27.36	0.27	10.75
	58.39	32	50.60	0.29	24.77
	58.39	40	60.83	0.30	33.06
6	58.39	0	6.21		
	58.39	8	19.28	0.21	9.40
	58.39	16	33.85	0.27	13.40
	58.39	24	33.05	0.28	12.92
	58.39	32	58.17	0.30	30.46
	58.39	40	75.11	0.33	41.94

Table 2. Data inputs to model for Amarillo soil.

RILL	INTENSITY mm/hr	INFLOW l/min	Q l/min/m	VELOCITY m/s	MEASURED SEDIMENT LOAD g/s/m
1	60.25	0	7.75		
	60.25	8	24.93	0.24	31.44
	60.25	16	40.42	0.28	54.04
	60.25	24	52.30	0.30	73.21
	60.25	32	68.51	0.35	123.75
	60.25	40	85.49	0.37	169.77
2	60.25	0	7.02		
	60.25	8	24.01	0.21	19.90
	60.25	16	38.96	0.28	48.88
	60.25	24	52.23	0.33	61.85
	60.25	32	66.28	0.37	81.33
	60.25	40	84.55	0.42	150.71
3	60.25	0	7.40		
	60.25	8	24.58	0.28	10.77
	60.25	16	42.02	0.29	14.98
	60.25	24	58.64	0.31	18.42
	60.25	32	72.64	0.35	21.71
	60.25	40	97.55	0.39	24.46
4	60.25	0	7.38		
	60.25	8	23.08	0.25	54.69
	60.25	16	39.91	0.30	49.38
	60.25	24	48.44	0.32	91.65
	60.25	32	64.22	0.36	140.10
	60.25	40	87.06	0.43	187.38
5	60.25	0	6.29		
	60.25	8	19.78	0.25	25.13
	60.25	16	38.09	0.26	42.19
	60.25	24	48.93	0.26	69.83
	60.25	32	66.19	0.33	108.23
	60.25	40	86.51	0.36	171.29
6	60.25	0	5.65		
	60.25	8	24.13	0.24	38.06
	60.25	16	36.03	0.25	50.85
	60.25	24	50.47	0.28	68.15
	60.25	32	63.97	0.35	76.52
	60.25	40	81.87	0.36	178.58

Table 3. Data inputs to model for Heiden soil.

RILL	INTENSITY mm/hr	INFLOW l/min	Q l/min/m	VELOCITY m/s	MEASURED SEDIMENT LOAD g/s/m
1	1	0	5.71		
	59.65	8	18.81	0.12	18.04
	59.65	16	34.71	0.15	39.48
	59.65	24	49.35	0.19	58.17
	59.65	32	67.94	0.21	67.13
	59.65	40	79.80	0.25	112.75
2	59.65	0	10.52		
	59.65	8	25.62	0.12	14.63
	59.65	16	41.57	0.15	21.52
	59.65	24	55.80	0.18	34.04
	59.65	32	71.84	0.20	34.73
	59.65	40	84.55	0.21	71.44
3	59.65	0	6.67		
	59.65	8	20.52	0.13	5.88
	59.65	16	34.75	0.15	23.58
	59.65	24	54.90	0.18	45.60
	59.65	32	66.32	0.21	68.73
	59.65	40	80.54	0.23	95.40
4	59.65	0	9.63		
	59.65	8	23.07	0.13	8.10
	59.65	16	37.64	0.14	21.85
	59.65	24	53.32	0.17	37.31
	59.65	32	67.40	0.18	39.60
	59.65	40	83.51	0.18	47.19
5	59.65	0	10.04		
	59.65	8	25.06	0.14	22.63
	59.65	16	43.40	0.22	38.48
	59.65	24	60.20	0.22	58.25
	59.65	32	74.94	0.23	79.90
	59.65	40	78.88	0.28	84.85
6	59.65	0	3.31		
	59.65	8	13.21	0.09	10.67
	59.65	16	31.85	0.15	35.92
	59.65	24	41.94	0.18	47.29
	59.65	32	58.67	0.16	81.77
	59.65	40	65.50	0.23	128.23

Table 4. Data inputs to model for Walla Walla soil.

RILL	INTENSITY	INFLOW	Q	VELOCITY	MEASURED SEDIMENT LOAD
	mm/hr	l/min	l/min/m	m/s	g/s/m
1	64.35	0	7.04		
	64.35	8	15.76	0.21	36.13
	64.35	16	38.53	0.27	97.81
	64.35	24	54.58	0.30	139.29
	64.35	32	68.85	0.32	230.15
	64.35	40	99.14	0.36	316.46
2	64.35	0	7.71		
	64.35	8	18.65	0.22	38.63
	64.35	16	38.09	0.30	100.54
	64.35	24	56.88	0.31	133.79
	64.35	32	74.50	0.34	219.79
	64.35	40	102.76	0.36	306.88
3	64.35	0	6.46		
	64.35	8	19.16	0.25	39.33
	64.35	16	37.96	0.29	86.42
	64.35	24	53.93	0.29	139.79
	64.35	32	69.96	0.28	223.15
	64.35	40	92.35	0.36	291.52
4	64.35	0	6.96		
	64.35	8	22.64	0.27	50.17
	64.35	16	38.52	0.25	87.21
	64.35	24	51.71	0.30	124.65
	64.35	32	65.01	0.29	174.33
	64.35	40	84.65	0.35	205.00
5	64.35	0	6.79		
	64.35	8	19.18	0.25	36.96
	64.35	16	37.96	0.25	85.44
	64.35	24	49.51	0.27	128.44
	64.35	32	62.91	0.32	219.15
	64.35	40	78.01	0.35	316.96
6	64.35	0	6.88		
	64.35	8	21.59	0.26	38.04
	64.35	16	40.38	0.27	88.17
	64.35	24	56.96	0.30	168.33
	64.35	32	71.04	0.34	212.83
	64.35	40	109.70	0.36	333.10

Table 5. Data inputs to model for Grant soil

PLOT	INTENSITY mm/hr	INFLOW mm/hr	Q l/min/m	MEASURED SEDIMENT LOAD g/s/m
72	55.27	0	9.05	1.05
	107.65	0	15.37	2.53
	55.92	0	9.23	1.34
	55.27	40	15.60	1.88
	55.27	85	21.62	2.02
	55.27	130	23.71	1.90
74	52.15	0	8.12	0.70
	91.67	0	13.78	1.45
	52.15	40	14.21	0.74
	51.34	85	20.94	0.92
	49.87	130	24.85	0.88

Table 6. Data inputs to model for Pratt soil

PLOT	INTENSITY mm/hr	INFLOW mm/hr	Q l/min/m	MEASURED SEDIMENT LOAD g/s/m
85	53.33	0	0.32	0.09
	100.31	0	4.67	1.16
	53.33	40	10.17	8.60
	53.33	85	14.48	13.86
	53.33	130	16.27	16.79
89	59.23	0	0.08	0.01
	102.59	0	4.81	1.20
	59.23	40	4.67	1.17
	59.23	85	10.06	3.13
	59.23	130	11.36	4.13

Table 7. Data inputs to model for Degater soil.

PLOT	INTENSITY mm/hr	INFLOW mm/hr	Q l/min/m	MEASURED SEDIMENT LOAD g/s/m
108	59.15	0	5.56	1.46
	109.85	0	11.98	6.40
	58.45	0	7.95	4.92
	58.45	40	12.20	8.88
	58.45	85	18.80	12.65
	57.95	130	27.56	30.26
	57.95	200	43.73	47.95
110	63.95	0	8.91	2.69
	133.41	0	19.91	9.24
	65.49	0	12.61	5.19
	65.49	40	21.66	7.95
	65.49	85	26.98	10.02
	65.49	130	30.36	10.06
	65.49	200	48.03	16.88

Table 8. Data inputs to model for Pierre soil.

PLOT	INTENSITY mm/hr	INFLOW mm/hr	Q l/min/m	MEASURED SEDIMENT LOAD g/s/m
114	53.61	0	8.77	4.26
	87.36	0	15.22	7.06
	52.15	0	8.77	3.29
	52.15	40	16.67	4.40
	52.15	85	22.95	5.84
	52.15	130	30.75	7.15
116	52.46	0	8.51	1.90
	103.35	0	15.97	4.68
	53.27	0	8.89	2.39
	52.46	40	19.89	4.36
	52.46	85	25.70	5.94
	51.54	130	26.00	6.79
	51.54	200	41.07	8.80

Table 9. Data inputs to model for Querencia soil.

PLOT	INTENSITY mm/hr	INFLOW mm/hr	Q l/min/m	MEASURED SEDIMENT LOAD g/s/m
131	51.72	0	7.45	0.49
	113.35	0	15.97	2.51
	52.59	0	7.92	0.78
	52.59	40	17.00	2.04
	52.59	85	22.71	3.23
	53.40	130	26.26	3.43
134	52.85	0	7.30	0.75
	109.70	0	17.55	3.58
	50.76	0	7.62	1.23
	50.76	40	19.94	2.54
	50.76	85	24.05	3.22
	50.76	130	23.77	2.11

APPENDIX B

Table 1. Measured and optimized sediment loads for Sharpsburg soil.

SEDIMENT LOADS

RILL	MEASURED g/s/m	3 PARAMETER RILL g/s/m	3 PARAMETER SHEET g/s/m	2 PARAMETER RILL g/s/m	2 PARAMETER SHEET g/s/m
1	9.81	8.96	10.58	5.53	5.97
	11.58	14.16	12.76	13.84	14.04
	12.92	13.98	12.56	13.64	13.83
	32.15	25.32	28.26	25.57	27.89
	32.06	35.59	35.42	35.88	34.34
2	10.54	8.32	11.73	9.31	8.27
	17.63	19.03	11.93	19.50	17.59
	14.42	19.22	12.17	19.67	18.00
	32.83	27.94	32.53	27.46	32.66
	39.81	40.63	41.24	40.42	38.84
3	7.44	6.64	3.23	5.52	5.52
	17.83	20.34	21.11	20.42	21.65
	27.63	26.29	24.52	26.29	24.97
	56.31	62.28	52.48	61.99	52.16
	67.40	61.29	71.07	61.23	70.25
4	5.29	5.45	9.96	5.53	5.53
	18.19	21.26	19.02	21.33	19.61
	17.19	18.53	20.22	18.60	20.77
	58.00	46.30	46.30	46.37	46.18
	59.92	66.89	67.07	66.96	66.52
5	11.71	12.22	12.53	5.82	8.15
	15.35	13.76	12.51	13.33	16.45
	10.75	12.52	12.52	10.98	14.40
	24.77	25.82	24.58	25.72	26.03
	33.06	32.41	33.14	32.32	30.58
6	9.40	10.78	12.12	5.52	5.52
	13.40	13.37	12.00	13.09	13.31
	12.92	13.03	12.10	12.66	12.79
	30.46	30.09	29.65	30.24	30.95
	41.94	41.98	42.08	42.32	41.70

Table 2. Measured and optimized sediment loads for Amarillo soil.

	SEDIMENT LOADS				
		3 PARAMETER		2 PARAMETER	
RILL	MEASURED g/s/m	RILL g/s/m	SHEET g/s/m	RILL g/s/m	SHEET g/s/m
1	31.44	26.56	17.30	24.83	23.04
	54.04	62.25	48.85	62.45	64.03
	73.21	87.41	84.33	87.75	89.65
	123.75	121.98	124.18	122.09	123.20
	169.77	158.85	163.34	158.56	157.57
2	19.90	13.67	13.67	13.64	13.35
	48.88	41.64	40.23	41.94	39.99
	61.85	70.10	71.22	70.22	71.01
	81.33	98.52	99.80	98.55	99.61
	150.71	135.12	134.80	135.06	134.61
4	54.69	37.85	39.63	37.85	40.12
	49.38	71.21	77.26	71.18	77.79
	91.65	89.43	96.62	89.39	97.06
	140.10	124.56	132.18	124.55	132.38
	187.38	175.46	183.71	175.41	183.48
5	25.13	25.78	23.91	13.36	13.36
	42.19	39.07	39.62	41.42	38.89
	69.83	75.17	75.07	74.67	74.30
	108.23	115.58	117.05	113.92	116.81
	171.29	159.46	162.25	157.64	162.87
6	38.06	30.79	27.80	37.06	28.58
	50.85	54.08	54.72	58.47	55.79
	68.15	82.02	83.90	86.09	84.46
	76.52	108.71	110.55	113.17	110.46
	178.58	144.96	145.44	150.46	144.36

Table 3. Measured and optimized sediment loads for Heiden soil.

	SEDIMENT LOADS				
		3 PARAMETER		2 PARAMETER	
RILL	MEASURED g/s/m	RILL g/s/m	SHEET g/s/m	RILL g/s/m	SHEET g/s/m
1	18.04	5.96	15.22	5.72	15.89
	39.48	17.10	39.72	17.04	39.55
	58.17	44.93	59.95	42.18	59.85
	67.13	68.37	83.85	66.64	83.86
	112.75	114.29	98.43	115.65	98.52
2	14.63	6.72	9.59	6.71	9.57
	21.52	16.49	24.57	16.31	24.77
	34.04	32.35	36.33	32.16	36.55
	34.73	49.61	48.52	49.50	48.74
	71.44	61.82	57.66	61.80	57.87
3	5.88	8.22	7.15	7.98	4.19
	23.58	17.06	20.30	17.00	20.17
	45.60	39.73	54.00	38.39	53.56
	68.73	67.34	70.46	67.35	69.98
	95.40	95.94	89.93	97.34	89.43
4	8.10	8.27	13.06	8.45	10.35
	21.85	14.13	22.43	14.13	21.33
	37.31	31.57	32.20	31.40	31.76
	39.60	42.71	40.21	42.51	40.31
	47.19	47.67	48.81	47.52	49.49
5	22.63	11.46	19.50	10.78	19.52
	38.48	47.67	42.90	47.26	42.92
	58.25	56.35	62.28	56.41	62.29
	79.90	70.38	78.18	70.88	78.20
	84.85	88.75	82.32	89.44	82.33

Table 4. Measured and optimized sediment loads for Walla Walla soil.

	SEDIMENT LOADS				
		3 PARAMETER		2 PARAMETER	
RILL	MEASURED	RILL	SHEET	RILL	SHEET
	g/s/m	g/s/m	g/s/m	g/s/m	g/s/m
1	36.13	30.48	24.51	29.93	14.44
	97.81	97.65	113.40	97.31	91.90
	139.29	158.04	168.38	157.82	158.50
	230.15	213.00	214.23	212.88	212.29
	316.46	319.41	307.19	319.49	320.66
2	38.63	28.81	30.76	29.44	30.15
	100.54	100.71	102.68	101.38	102.36
	133.79	157.62	161.46	157.88	161.14
	219.79	212.97	215.45	213.05	215.12
	306.88	300.49	297.08	300.42	296.70
3	39.33	43.13	29.23	42.30	14.43
	86.42	106.77	104.85	107.06	83.39
	139.79	162.05	159.29	162.45	151.41
	223.15	175.88	211.90	175.21	212.47
	291.52	298.53	283.20	299.35	294.12
4	50.17	62.91	48.07	60.74	47.81
	87.21	81.55	93.40	79.63	93.59
	124.65	135.27	128.43	134.82	128.49
	174.33	149.85	162.09	149.70	161.95
	205.00	213.52	209.49	215.59	209.07
5	36.96	31.95	15.39	28.74	14.43
	85.44	82.07	80.26	98.95	79.98
	128.44	156.25	157.96	156.05	157.94
	219.15	223.23	223.00	220.45	223.05
	316.96	286.06	291.10	282.50	291.21
6	38.04	36.56	34.77	36.37	34.06
	88.17	103.53	107.58	103.97	107.76
	168.33	157.84	162.29	158.17	162.52
	212.83	204.76	208.18	204.93	208.41
	333.10	337.65	332.64	337.29	332.83

Table 5. Measured and optimized sediment loads for Grant soil.

	SEDIMENT LOADS				
		3 PARAMETER		2 PARAMETER	
PLOT	MEASURED g/s/m	RILL g/s/m	SHEET g/s/m	RILL g/s/m	SHEET g/s/m
72	1.05	1.26	1.27	2.62	2.62
	2.53	2.59	2.57	2.51	2.52
	1.34	1.29	1.30	2.68	2.68
	1.88	1.54	1.53	2.60	2.60
	2.02	1.95	1.96	2.60	2.61
	1.90	2.08	2.08	2.60	2.60
74	0.70	0.71	0.68	2.33	2.33
	1.45	1.44	1.45	1.43	1.45
	0.74	0.79	0.78	2.31	2.31
	0.92	0.87	0.88	2.23	2.24
	0.88	0.90	0.91	2.13	2.13

Table 6. Measured and optimized sediment loads for Pratt soil.

	SEDIMENT LOADS				
		3 PARAMETER		2 PARAMETER	
PLOT	MEASURED g/s/m	RILL g/s/m	SHEET g/s/m	RILL g/s/m	SHEET g/s/m
85	0.09	0.06	0.32	0.13	0.13
	1.16	1.17	1.11	1.20	0.89
	8.60	8.48	7.98	8.40	8.93
	13.86	14.21	14.38	14.20	14.18
	16.79	16.61	16.84	16.62	16.22
89	0.01	0.23	0.01	0.16	0.03
	1.20	1.42	1.21	1.34	1.35
	1.17	0.47	1.13	0.99	0.97
	3.13	3.13	3.42	3.37	3.40
	4.13	4.13	3.91	3.95	3.91

Table 7. Measured and optimized sediment loads for Degater soil.

	SEDIMENT LOADS				
		3 PARAMETER		2 PARAMETER	
PLOT	MEASURED g/s/m	RILL g/s/m	SHEET g/s/m	RILL g/s/m	SHEET g/s/m
108	1.46	0.12	0.14	0.25	0.01
	6.40	7.18	5.92	7.19	10.32
	4.92	4.97	2.49	4.75	4.98
	8.88	7.18	7.33	7.13	8.94
	12.65	15.25	17.29	15.35	18.22
	30.26	27.25	28.78	27.31	29.01
	47.95	48.96	47.55	48.92	46.66
110	2.69	1.08	1.61	0.52	0.01
	9.24	10.06	9.84	10.22	13.41
	5.19	4.70	3.74	5.69	5.70
	7.95	6.98	7.57	7.29	7.95
	10.02	9.13	9.68	9.16	9.83
	10.06	10.48	10.93	10.44	10.94
	16.88	17.40	16.74	17.02	16.12

Table 8. Measured and optimized sediment loads for Pierre soil.

	SEDIMENT LOADS				
		3 PARAMETER		2 PARAMETER	
PLOT	MEASURED g/s/m	RILL g/s/m	SHEET g/s/m	RILL g/s/m	SHEET g/s/m
114	4.26	3.14	3.21	3.08	3.36
	7.06	7.48	7.37	7.67	7.87
	3.29	3.09	3.18	3.10	3.32
	4.40	4.70	4.85	4.69	4.91
	5.84	5.83	5.89	5.81	5.89
	7.15	7.09	6.97	7.08	6.91
116	1.90	1.87	2.09	2.36	2.25
	4.68	4.83	4.87	4.90	4.85
	2.39	1.97	2.17	2.45	2.33
	4.36	4.67	4.46	4.38	4.49
	5.94	5.92	5.88	5.73	5.93
	6.79	6.01	5.95	5.79	5.99
	8.80	9.19	9.25	9.35	9.34

Table 9. Measured and optimized sediment loads for Querencia soil.

	SEDIMENT LOADS				
		3 PARAMETER		2 PARAMETER	
PLOT	MEASURED	RILL	SHEET	RILL	SHEET
	g/s/m	g/s/m	g/s/m	g/s/m	g/s/m
131	0.49	0.55	0.43	0.27	0.00
	2.51	2.50	2.53	2.61	2.72
	0.78	0.80	0.71	1.00	0.94
	2.04	2.15	2.19	2.04	2.04
	3.23	3.01	3.03	3.00	3.02
	3.43	3.55	3.51	3.61	3.59
134	0.75	0.80	0.90	0.47	0.49
	3.58	3.64	3.61	4.58	4.68
	1.23	0.93	0.99	0.97	0.98
	2.54	2.36	2.39	2.22	2.25
	3.22	2.79	2.74	2.67	2.62
	2.11	2.76	2.72	2.64	2.60

LIST OF REFERENCES

Blau, J. B., D. A. Woolhiser, and L. J. Lane. 1988. Identification of erosion model parameters. Accepted for publication. Transactions of the ASAE.

Brown, L. C. 1988. Effects of incorporated crop residue on rill erosion. Ph.D. Thesis, Purdue University. W. Lafayette, IN. 197 pp.

Foster, G. R. 1971. The overland flow process under natural conditions. pp. 173-185. In: Biological effects in the Hydrological Cycle. E. J. Monke (ed.). Proceedings of the Third International Seminar for Hydrology Professors; Department of Agricultural Engineering, Purdue University, West Lafayette, IN.

Foster, G. R. 1982. Modeling the erosion process. pp. 297-380. In: Hydrologic Modeling of Small Watersheds. C. T. Haan, H. P. Johnson, and D. L. Brakensiek, (eds.) ASAE monograph No. 5. ASAE, St. Joseph, MI.

Foster, G. R., L. F. Huggins, and L. D. Meyer. 1984a. A laboratory study of rill hydraulics: I. Velocity relationships. Transactions of the ASAE, 27(3):790-796.

Foster, G. R., L. F. Huggins, and L. D. Meyer. 1984b. A laboratory study of rill hydraulics: II. Shear stress relationships. Transactions of the ASAE, 27(3):797-804.

Foster, G. R., and L. J. Lane. 1987. User Requirements: USDA- Water Erosion Predection Project (WEPP). NSERL Report No. 1. National Soil Erosion Research Laboratory, USDA-ARS, W. Lafayette, IN, 43 pp.

Foster, G. R., L. J. Lane, D. L. Shertz, J. O. Nordin, and G. D. Wingate. 1987. User requirements: USDA-Water erosion prediction project (WEPP). ASAE paper 87-2539. Winter 1987 ASAE meeting, Chicago IL.

Foster, G. R. and L. D. Meyer. 1972. A closed-form soil erosion equation for upland areas. Sedimentation, Proceedings Symposium to Honor Professor H. A. Einstein, H. W. Shen, editor and publisher, Colorodo State University, Ft. Collins, Colorado.

Foster, G. R., and L. D. Meyer. 1975. Mathematical simulation of upland erosion by fundamental erosion mechanics. In: Present and Prospective Technology for Predicting Sediment Yields and Sources, USDA-Agricultural Research Service, ARS-S-40, pp. 191-207.

Foster, G. R., L. D. Meyer, and C. A. Onstad. 1977. An erosion equation derived from basic erosion principles. Transactions of the ASAE, 20(4):678-682.

Freeze, R. A. 1978. Mathematical models of hillslope hydrology. In: Hillslope Hydrology. M. J. Kirkby (ed.) John Wiley and Sons, New York, NY. pp. 117-225.

Gilley, J. E., S. C. Finkner, R. G. Spomer, and L. N. Mielke. 1986a. Runoff and erosion as affected by corn residue: Part I. Total losses. Transactions of the ASAE, 29(1):157-160.

Gilley, J. E., S. C. Finkner, R. G. Spomer, and L. N. Mielke. 1986b. Runoff and erosion as affected by corn residue: Part II. Rill and interrill components. Transactions of the ASAE, 29(1):161-164.

Gilley, J. E., S. C. Finkner, and G. E. Varvel. 1987. Slope length and surface residue influences on runoff and erosion. Transactions of the ASAE, 30(1):148-152.

Graf, W. H. 1971. Hydraulics of sediment transport. McGraw- Hill Book Co., New York, NY. 544 pp.

Horton, R. E. 1945. Erosional developmenmt of streams and their drainage basins; Hydrophysical approach to quantitative morphology. Bulletin of the Geological Society of America, 56:275-370.

Hudson, N. W. 1981. Soil Conservation. Cornell University Press, Ithaca, New York, 324 pp.

Knisel, W. G. (ed.) 1980. CREAMS: A field-scale model for chemicals, runoff and erosion from agricultural management systems. USDA Conservation Research Report No. 26, USDA-SEA, Washington, D. C., 640 pp.

Laflen, J. M., A. W. Thomas and R. Welch. 1987. Cropland experiments for the WEPP project. ASAE paper no. 87-2544. Winter 1987 ASAE meeting, Chicago, IL.

Lane, L. J. and G. R. Foster. 1980a. Concentrated flow relationships. In: CREAMS-A field scale model for chemicals, runoff, and erosion from agricultural management systems. Volume III: Supporting Documentation. Chapter 11. USDA Conservation Report No. 26, USDA-SEA, Washington, D. C., pp. 474-485.

Lane, L. J. and G. R. Foster. 1980b. Modeling channel processes with changing land use. Proceedings of the Symposium on Watershed Management 1980. ASCE Boise, ID. July 21-23, 1980.

Lane, L. J., G. R. Foster, and A. D. Nicks. 1987. Use of fundamental erosion mechanics in erosion prediction. ASAE paper no. 87-2540. Winter 1987 ASAE meeting, Chicago, IL.

Lane, L. J., E. D. Shirley, and V. P. Singh. 1988. Modelling erosion on hillslopes. In: Modelling Geomorphological Systems. M. G. Anderson (ed.). Chapter 10. John Wiley and Sons Ltd. New York, N.Y. pp. 287-308.

Lane, L. J. and D. A. Woolhiser. 1977. Simplifications of watersheds geometry affecting simulation of surface runoff. Journal of Hydrology, 35:173-190.

Lattanzi, A. R., L. D. Meyer, and M. F. Baumgardner. 1974. Influences of mulch rate and slope steepness on interrill erosion. Soil Science Society of America Proceedings, 38(6):946-950.

Meyer, L. D., G. R. Foster, and S. Nikolov. 1975a. Effect of flow rate and canopy on rill erosion. Transactions of the ASAE, 18(5):905-911.

Meyer, L. D., G. R. Foster, and M. J. M. Romkens. 1975b. Source of soil eroded by water from upland slopes. In: Present and Prospective Technology for Predicting Sediment Yields and Sources, USDA-Agricultural Research Service, ARS-S-40, pp.177-189.

Meyer, L. D. and W. H. Wischmeier. 1969. Mathematical simulation of the process of soil erosion by water. Transactions of the ASAE, 12(6):754-758.

Nearing, M. A. In: WEPP Hillslope Model Documentation. L. J. Lane and M. A. Nearing (compilers). Chapter 10. unpublished manuscript USDA-ARS.

Nearing, M. A., L. J. Lane, D. I. Page, L, C. Brown, J. R. Simanton, and J. M. Laflen. Determining erodibility parameters for a process based erosion prediction model from field data. Unpublished manuscript. USDA-ARS, Tucson, AZ.

Rohlf, R. A. and M. E. Meadows. 1980. Dynamic mathematical modeling of rill erosion. Symposium on Watershed Management 1980. ASCE Boise, ID 1:13-26.

Rowlinson, D. L. and G. L. Martin. 1971. Rational model describing slope erosion. Journal of the Irrigation and Drainage Division, Proceedings of the American Society of Civil Engineers, 97(IR1):39-50.

Shirley, E. D. and L. J. Lane. 1978. A sediment yield equation from an erosion simulation model. Hydrology and Water Resources in Arizona and the Southwest, 8:90-96.

Simanton, J. R., M. A. Weltz, L. T. West, and G. D. Wingate. 1987. Rangeland experiments for water erosion prediction project. ASAE paper no. 87-2545. Winter 1987 ASAE meeting, Chicago, IL.

Smith, D. D. 1941. Interpretation of soil conservation data for field use. Agricultural Engineering 22:173-175.

Sorooshian, S. and F. Arfi. 1982. Response surface parameter sensitivity analysis methods for postcalibration studies. Water Resources Research, 18(5):1531-1538.

Swanson, N. P. 1965. Rotating-boom rainfall simulator. Transactions of the ASAE, 8(1):71-72.

Watson, D. A. and J. M. Laflen. 1986. Soil strength, slope and rainfall intensity effects on interrill erosion. Transactions of the ASAE, 29(1):98-102.

Wischmeier, W. H. and D. D. Smith. 1978. Predicting rainfall erosion losses-a guide to conservation planning. USDA Agriculture Handbook No. 537. 58 pp.

Woolhiser, D. A. and J. A. Liggett. 1967. Unsteady, one- dimensional flow over a plane-The rising hydrograph. Water Resources Research, 3(3):753-771.

Young, R. A., and C. K. Mutchler. 1969. Soil movement on irregular slopes. Water Resources Research, 5(1):184-189.

Young, R. A., and J. W. Wiersma. 1973. The role of rainfall impact on soil detachment and transport. Water Resources Research, 9:1629-1636.

Zingg, A. W. 1940. Degree and length of land slope as it affects soil loss in runoff. Agricultural Engineering 21:59-64.